

A photometric and spectroscopic survey of solar twin stars within 50 parsecs of the Sun:

I. Atmospheric parameters and color similarity to the Sun

G. F. Porto de Mello¹, R. da Silva^{1,*}, L. da Silva² and R. V. de Nader^{1,**}

¹ Universidade Federal do Rio de Janeiro, Observatório do Valongo, Ladeira do Pedro Antonio 43, CEP: 20080-090 Rio de Janeiro, RJ, Brazil

e-mail: gustavo@astro.ufrj.br, ronaldo.dasilva@oa-roma.inaf.it, rvnader@astro.ufrj.br

² Observatório Nacional, Rua Gen. José Cristino 77, CEP: 20921-400, Rio de Janeiro, Brazil

e-mail: licio@on.br

Received; accepted

ABSTRACT

Context. Solar twins and analogs are fundamental in the characterization of the Sun's place in the context of stellar measurements, as they are in understanding how typical the solar properties are in its neighborhood. They are also important for representing sunlight observable in the night sky for diverse photometric and spectroscopic tasks, besides being natural candidates for harboring planetary systems similar to ours and possibly even life-bearing environments.

Aims. We report a photometric and spectroscopic survey of solar twin stars within 50 parsecs of the Sun. Hipparcos absolute magnitudes and $(B - V)^{\text{Tycho}}$ colors were used to define a 2σ box around the solar values, where 133 stars were considered. Additional stars resembling the solar UBV colors in a broad sense, plus stars present in the lists of Hardorp, were also selected. All objects were ranked by a color-similarity index with respect to the Sun, defined by $uvby$ and BV photometry.

Methods. Moderately high-resolution, high-S/N spectra were used for a subsample of equatorial-southern stars to derive T_{eff} , $\log g$ (both ionization and evolutionary), and spectroscopic $[\text{Fe}/\text{H}]$ with average internal errors better than 50 K, 0.20 dex, and 0.08 dex, respectively. Ages and masses were estimated from theoretical HR diagrams.

Results. The color-similarity index proved very successful, since none of the best solar-analog and twin candidates that were photometrically and spectroscopically found to be good solar matches differed from the Sun by more than 3σ in their colors. We identify and quantitatively rank many new excellent solar analogs, which are fit to represent the Sun in the night sky to varying degrees of accuracy and in a wide range of contexts. Some of them are faint enough ($V^{\text{Tycho}} \sim 8.5$) to be of interest for moderately large telescopes. We also identify two stars with near-UV spectra indistinguishable from the Sun's, although only HD 140690 also has atmospheric parameters matching the Sun's, besides a high degree of photometric fidelity. This object is proposed as a prime solar analog in both the UV and visible ranges, a rare object. We present five new "probable" solar twin stars, besides five new "possible" twins, the best candidates being HD 98649, HD 118598, HD 150248, and HD 164595. Masses and isochronal ages for the best solar twin candidates lie very close to the solar values within uncertainties, but chromospheric activity levels range somewhat. We propose that the solar twins be emphasized in the ongoing searches for extra-solar planets and SETI searches.

Key words. Stars: solar analogs – Stars: atmospheres – Stars: abundances – Stars: late-type – Galaxy: solar neighborhood – Techniques: spectroscopy

1. Introduction

The Sun occupies a very special place in stellar studies, being still the most fundamental and dependable reference object in stellar astrophysics. It remains the one star for which extremely important parameters can be determined from first principles, such as the effective temperature T_{eff} from directly observed irradiance (Neckel 1986), age from nucleochronology and/or undisturbed meteorite differentiates (Guenther 1989;

Gancarz & Wasserburg 1977), and mass from planetary motion and asteroseismology. Nevertheless, to fully exploit the potential reference position of the Sun as a star, we need to know its place in the parameter space of stellar observations. This is no easy task: the extremely detailed observations available for the Sun are only tied with difficulty to the woefully less detailed stellar measurements. The main reasons for this in photometry and spectrophotometry are the difficulties in geometrically treating the solar image and scattered light; the immense flux difference between the Sun and stars, a factor of $\sim 10^{11}$; and the impossibility of observing the Sun at night, which taxes the stability of instrumentation. The photometric properties of the Sun in the various photometric systems in use, thus, remain uncertain despite protracted efforts employing a variety of direct and indirect methods (e.g., Tüg & Schmidt-Kaler 1982; Hayes 1985; Saxner & Hammarbäck 1985; Neckel 1986; Friel et al. 1993; Gray 1992, 1994; Porto de Mello & da Silva

Send offprint requests to: G. F. Porto de Mello, gustavo@astro.ufrj.br

* Present address: INAF, Osservatorio Astronomico di Roma, 00040, Monte Porzio Catone, Italy

** Based on spectroscopic observations collected at the Observatório do Pico dos Dias (OPD), operated by the Laboratório Nacional de Astrofísica, CNPq, Brazil, and the European Southern Observatory (ESO), within the ON/ESO and ON/IAG agreements, under FAPESP project n° 1998/10138-8.

1997; Ramírez & Meléndez 2005b; Holmberg et al. 2006; Casagrande et al. 2006; Meléndez et al. 2010, and many others).

The identification of stars closely resembling the Sun plays an extremely interesting role in this task (Cayrel de Strobel 1996) and raises considerable interest on diverse astrophysical fronts. Solar twin stars were defined by Cayrel de Strobel & Bentolila (1989) as (non binary) stars identical to the Sun, within the observational uncertainties, in all fundamental astrophysical parameters, such as mass, chemical composition, T_{eff} , surface gravity, photospheric velocity fields, magnetic activity, age, luminosity, and asteroseismological properties. Such stars should have spectra that are indistinguishable from the solar one. It is debatable whether such stars should be detectable, or even actually exist (Cayrel de Strobel et al. 1981). Even though uncertainties in determining fundamental stellar parameters have been decreasing steadily, minute differences from star to star may simply be too small to be distinguished. For instance, very slight variances in chemical composition or details of internal structure between two stars can lead to sizable disparities of observable spectral properties and evolutionary states, and turn them into very dissimilar objects indeed.

Solar analogs, by contrast, are unevolved, or hardly evolved, solar-type stars that merely share the solar atmospheric parameters and are thus expected to have very similar colors and spectral flux distributions to the Sun. We feel the distinction between solar twins and analogs has not been sufficiently stressed in the literature, and we thus take some time to point out some key issues. Solar twins, on the one hand, are expected to match every conceivable solar physical property, and therefore to materialize in a star all the photometric and spectroscopic solar properties, under the reasonable assumption that a perfect physical match would automatically lead to the same observables. Solar analogs, on the other hand, merely have the atmospheric parameters loosely similar to the solar ones, to degrees of similarity that have been taken at different values by different authors (alas, adding to the confusion). Such stars are expected to possess spectrophotometric quantities, including colors, similar to the solar ones, but we note that, due to the various degeneracies of the problem, which we discuss below, stars with colors resembling the Sun may not turn out to be solar analogs.

Solar analogs, and of course also solar twins, may be very useful in providing a proxy for sunlight in the night sky specifically for spectrophotometry of solar system bodies and other calibration purposes. These solar surrogates are very important for those cases when techniques that can be applied in daytime, such as observing the clear blue sky or solar radiation reflected off telescope domes, are not an option. Ideally these solar analogs should be faint enough for adequate use by large telescopes, and be observable with the same instrumentation as used for working with very faint targets, such as small and distant asteroids, besides being observable without the need of stoppers or neutral density filters, which always add some measure of uncertainty. Additionally, both solar twins and solar analogs are expected to help pin down the solar color indices better.

Moreover, solar twins may be expected to have followed an evolutionary history similar to that of the Sun. There is some evidence that the Sun may be metal-richer than the average G-type thin disk star in its neighborhood (Rocha-Pinto & Maciel 1996), though we note that recent data has cast doubt upon this claim, as judged by a revised solar (Asplund et al. 2009) and interstellar medium (Nieva & Przybilla 2012) composition, as well as results from nearby solar-type stars (Adibekyan et al.

2013). It also seems to be part of a stellar population that is heavily depleted in lithium (e.g., Pasquini et al. 1994; Takeda et al. 2007), and it may possess lower-than-average chromospheric activity for its age (Hall & Lockwood 2000; Hall et al. 2007), have more subdued photometric variability than stars with similar properties (Lockwood et al. 2007; Radick et al. 1998) (but see Hall et al. 2009), and have a slightly longer rotational period than stars of the same age (Pace & Pasquini 2004). In addition, the Sun seems to lead most of the local stars of similar age and metallicity in the velocity component towards the galactic rotation (Cayrel de Strobel 1996; Porto de Mello et al. 2006). Adding to these putative peculiarities (for an interesting review of this topic, see Gustafsson 1998), the Sun occupies a position very close to the Galactic corotation (Lépine et al. 2001), whereby the Sun shares the rotational velocity of the spiral arms and the number of passages through them is presumably minimized. These characteristics may have a bearing on the Sun's ability to maintain Earth's biosphere on long timescales (Leitch & Vasisht 1998; Gonzalez et al. 2001; Porto de Mello et al. 2009).

Is the Sun an atypical star for its age and galactic position? A sample of nearby solar twins may help gauge the solar status in the local population of middle-aged G-type stars better. And, last but not least, solar twin stars would be natural choices when searching for planetary systems similar to our own, as well as presenting interesting targets to the ongoing SETI programs (Tarter 2001) and the planned interferometric probes aimed at detecting life, remotely, in extra solar Earth-like planets by way of biomarkers (Segura et al. 2003).

The search for solar analogs was initially stimulated by Hardorp (1982, and references therein) when attempting to identify stars with UV spectra matching the solar one, as judged mainly by the CN feature around $\lambda 3870$. Hardorp classed stars by magnitude differences of their spectral features to the Sun's (represented by Galilean satellites), and his solar analog lists are still widely referred to nowadays (e.g., Alvarez-Candal et al. 2007; Milani et al. 2006). This prompted an effort by Cayrel de Strobel et al. (1981), Cayrel de Strobel & Bentolila (1989), and Friel et al. (1993) to check that Hardorp's best candidates stood up to detailed spectroscopic analysis: this subject received a thorough review by Cayrel de Strobel (1996). Subsequently, Porto de Mello & da Silva (1997) used a detailed spectroscopic and evolutionary state analysis to show that 18 Sco (HR 6060, HD 146233) was a nearly perfect match for the Sun as judged by colors, chemical composition, T_{eff} , surface gravity, luminosity, mass, and age, thereby confirming that the 16 Cyg A and B pair (HD 186408 and HD 186427), previously pointed to by the Cayrel de Strobel group as the best solar twins, were older, less active, and more luminous than the Sun, though possessing T_{eff} and metallicity very near the Sun's. Glushneva et al. (2000) analyzed the spectral energy distributions of solar analogs from Hardorp's lists, concluding that 16 Cyg A and B are the closest matches to the solar distribution, followed closely by 18 Sco, but, as did Porto de Mello & da Silva (1997), they found the two former objects to be more luminous than the Sun, concluding that they are not true solar twins. Soubiran & Triaud (2004) have analyzed moderately high-resolution, homogeneous ELODIE spectra by comparing the stars with spectra of Moon and Ceres in an automated χ^2 method measuring over 30 000 resolution elements. They confirm that HD 146233 is the best match for the Sun and conclude that both photometric and spectroscopic data must be assembled to find real solar twins. These authors also found a very large dispersion in the published at-

mospheric parameters of solar analog candidates. Galeev et al. (2004) have spectroscopically analyzed 15 photometric analogs of the Sun, presenting HD 146233 and HD 186427 as the best analogs, along with HD 10307 and HD 34411, also concurring that photometric and spectroscopic data must be merged for a precise determination of similarity to the Sun.

King et al. (2005) suggest that HD 143436 is as good a solar twin as HD 146233. Meléndez et al. (2006) present HD 98618 as another star as close to the solar properties as HD 146233, and Meléndez et al. (2007) claim that the best solar twins ever are HD 101364 and HD 133600, since they not only reproduce all the solar fundamental parameters but also have a similar lithium abundance (see also Meléndez et al. 2012). Takeda et al. (2007) draw attention to the importance of the lithium abundance as a record of the stellar history of mixing and rotational evolution, concluding that slow rotation induces greater depletion. Finally, do Nascimento Jr. et al. (2009) show that the lithium depletion history of solar analogs is critically mass-dependent and suggest that, among the proposed solar twins, the best match for the solar convective properties, including the Li abundance, is HD 98618. This star also seems to fit the solar mass and age very closely. Israelian et al. (2004, 2009) suggest that an enhanced depletion of lithium is linked to the presence of planetary companions; however, this claim has been questioned by Luck & Heiter (2006), Ghezzi et al. (2010), and Baumann et al. (2010). It is possible that the very low lithium abundance of the Sun and other stars may be yet another piece of the major observational and theoretical puzzle of planetary formation.

As part of an ongoing effort at a complete survey of solar analog stars nearer than 50 pc, this paper reports a volume-limited, homogeneous, and systematic photometric and spectroscopic survey of solar twin stars, approximately restricted to $\delta \leq +30^\circ$ in what pertains to spectroscopic observations. It is, however, photometrically complete and all-sky within $d \leq 40$ pc and $V^{\text{Tycho}} \leq 8$, and partially complete (owing to lack of photometry) within $40 \text{ pc} < d < 50 \text{ pc}$ and $8 < V^{\text{Tycho}} < 9$. The best candidates will be subjected to detailed spectroscopic analysis that employs higher resolution spectra in a forthcoming paper. In section 2 the selection of the sample is described. In section 3 we describe the results of the photometric similarity analysis. In section 4 the observational data are presented, and the spectroscopic analysis is described in section 5. In section 6 we discuss the spectroscopic results and obtain masses and ages in an evolutionary analysis, presenting the best candidates, and we draw the conclusions in section 7. A new photometric calibration of T_{eff} on colors and metallicity, based on IRFM data and tailored specifically to solar analog stars and MARCS model atmosphere analysis, is presented in the Appendix.

2. Sample selection

In a solar-analog hunt, by the very nature of the objects, the selection of candidates must be initiated photometrically by colors and absolute magnitudes. The next step in the selection process must be spectroscopic, since atmospheric parameters and luminosities of the candidate objects will be compared to those of the Sun. An important question, therefore, is the availability of consistent T_{eff} scales where the Sun may be accurately placed both photometrically and spectroscopically.

Porto de Mello et al. (2008) discussed, in their analysis of the atmospheric parameters of the α Centauri binary system, possible offsets between the various published photometric and spectroscopic T_{eff} scales. While one conclusion was that there is

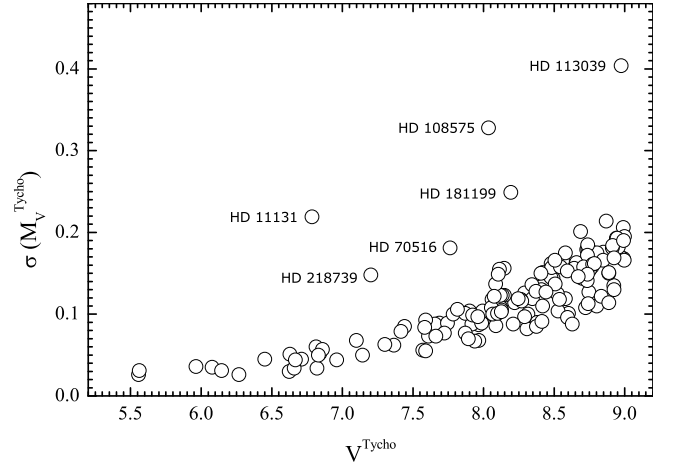


Fig. 1. Uncertainties in the M_V^{Tycho} absolute magnitudes for stars of the final sample of 158 non-binary stars selected from the Hipparcos catalog. Outliers with large errors in absolute magnitude are identified by HD numbers.

no consensus as yet on the existence of inconsistencies between the two scales, there is evidence that for stars that are substantially cooler than the Sun, $T_{\text{eff}} \leq 5300 \text{ K}$, NLTE, and other effects may be precluding strict consistency between them (e.g., Yong et al. 2004). For stars with T_{eff} that are not too dissimilar from the Sun, good agreement can be expected between photometric and spectroscopic T_{eff} s. This is an important issue, since the properties of solar twins and analogs must be equal to those of the Sun in a variety of contexts, such as in narrow and broad-band photometry and in low and high-resolution spectroscopy. On the other hand, a differential spectroscopic approach allows direct comparison between Sun and stars.

In the appendix, we present a new photometric calibration for solar-type stars for many colors in regular use, including the $(B - V)_{\text{Johnson}}$, $(B - V)_{\text{Tycho}}$, and Strömgren $(b - y)$ indices, based on published T_{eff} s employing the infrared flux method. The Paschen continuum colors have been metallicity-calibrated using only spectroscopic metallicities from detailed analyses. Our solar twin selection process starts from the Hipparcos catalog (ESA 1997) photometry and is subsequently refined with $(B - V)$ and Strömgren color indices. From the calibrations described in the Appendix, solar color indices were derived and have been the basis for our selection of solar twin candidates.

From our photometric calibrations, adopting for the Sun $T_{\text{eff}} = 5777 \text{ K}$ (Neckel 1986), we obtain

$$(B - V)_{\odot}^{\text{Johnson}} = 0.653$$

$$(B - V)_{\odot}^{\text{Tycho}} = 0.737$$

$$(b - y)_{\odot} = 0.409.$$

These values are in good agreement, within quoted errors, with the determinations of Holmberg et al. (2006) and Casagrande et al. (2010), for all three colors, and with $(b - y)_{\odot}$ as given by Meléndez et al. (2010).

For the m_1 index, we adopted the same procedure as employed by Porto de Mello & da Silva (1997) to derive the solar $(B - V)$ and $(U - B)$ colors. A sample of nine stars, spectroscopically analyzed with homogeneous methods, with solar metallicity, and a narrow range of T_{eff} s around the Sun leads to,

interpolating the solar T_{eff} in an m_1 versus T_{eff} regression:

$$m_1^\odot = 0.217 \text{ (F catalog; see below).}$$

This same procedure was applied to the Paschen continuum colors and led to $(B - V)_\odot^{\text{Johnson}} = 0.648$, $(B - V)_\odot^{\text{Tycho}} = 0.730$, and $(b - y)_\odot = 0.406$, in excellent agreement with the solar colors derived directly from the photometric calibrations. Our m_1^\odot also agrees very well with the recent derivation of Meléndez et al. (2010).

The initial selection process sets up a 2σ box around the $(B - V)_\odot^{\text{Tycho}}$ and the solar absolute magnitude in the Tycho system, $M_{V_\odot}^{\text{Tycho}}$. To obtain the latter figure, we compared the Sun to the solar twin HD 146233 (18 Sco) (Porto de Mello & da Silva 1997), and set

$$M_{V_{18 \text{ Sco}}}^{\text{Tycho}} - M_{V_\odot}^{\text{Tycho}} = M_{V_{18 \text{ Sco}}}^{\text{Johnson}} - M_{V_\odot}^{\text{Johnson}}.$$

Regarding the similarity between the V and V^{Tycho} bands and the very slight absolute magnitude difference between the Sun and HD 146233 in the Johnson V band, this procedure should not introduce any systematic error. We take $M_{V_\odot} = 4.82$ (Neckel 1986), and from the Hipparcos parallax obtain $M_{V_{18 \text{ Sco}}}^{\text{Johnson}} = 4.77$ and $M_{V_{18 \text{ Sco}}}^{\text{Tycho}} = 4.83$, to derive $M_{V_\odot}^{\text{Tycho}} = 4.88 \pm 0.03$, to which we formally attach the uncertainty of $M_{V_{18 \text{ Sco}}}^{\text{Tycho}}$.

The widths of the 2σ $(B - V)^{\text{Tycho}}$ vs. $M_{V_\odot}^{\text{Tycho}}$ box were arrived at by an iterative procedure. The uncertainties in $(B - V)^{\text{Tycho}}$ and $M_{V_\odot}^{\text{Tycho}}$, are obtained from the uncertainties of the B^{Tycho} and V^{Tycho} bands respectively, and the uncertainty in the parallax and the V^{Tycho} band. Experimentation with arbitrary widths revealed that the average uncertainties were a function of the magnitude limit, being independent of the absolute magnitude and color indices of the selected stars. The Hipparcos catalog is formally complete down to $V^{\text{Tycho}} \sim 9.0$, an apparent magnitude that translates to a distance of 67 parsecs for a star with the same luminosity as the Sun. The uncertainty in $M_{V_\odot}^{\text{Tycho}}$ increases smoothly as magnitude increases, and there is a small discontinuity at $V^{\text{Tycho}} \sim 8.0$ (Fig. 1). At this magnitude, approximately, the completeness limit of the *uvby* catalogs also lies (Olsen 1983, 1993, 1994a,b); indeed, the completeness of these catalogs was lost at $V^{\text{Tycho}} \sim 8.1$, for the samples selected in the first iterative runs. Our sample was therefore divided at $V^{\text{Tycho}} = 8.0$. The 2σ limits of the box were chosen so that the box widths corresponded to the average uncertainties of the $(B - V)^{\text{Tycho}}$ and $M_{V_\odot}^{\text{Tycho}}$ for the stars inside the box. This was satisfied by $\langle \sigma \rangle (M_{V_\odot}^{\text{Tycho}}) = 0.07$ and $\langle \sigma \rangle ((B - V)^{\text{Tycho}}) = 0.013$, for $V^{\text{Tycho}} \leq 8.0$ stars. The corresponding values for the $8.0 < V^{\text{Tycho}} < 9.0$ stars are 0.013 and 0.020, respectively, but the figures for $V^{\text{Tycho}} \leq 8.0$ stars were used to define both boxes. We chose to enforce strict consistency for the brighter sample, for which *uvby* photometry is complete and for which better spectroscopic data could be secured. After binary or suspected binary stars were removed from the list, 158 stars were retained, 52 having $V^{\text{Tycho}} \leq 8.0$. The completeness of the availability of the $(B - V)^{\text{Tycho}}$ color in the Hipparcos catalog for $V^{\text{Tycho}} \leq 8.0$ stars of all spectral types is 92%. This figure increases to 95% for G-type stars. A 2σ box is thus seen to be a practical limit that allows the working sample to be observed spectroscopically in a reasonable amount of time.

To this sample we added some stars selected in the Bright Star Catalog (Hoffleit & Jaschek 1991; Hoffleit 1991) solely for

having both $(B - V)$ and $(U - B)$ colors similar to the solar ones, plus a few stars from Hardorp (1982). For the solar colors, we used $(B - V)^\odot = 0.653 \pm 0.003$ (as above) and $(U - B)^\odot = 0.178 \pm 0.013$ (the latter from Porto de Mello & da Silva 1997). Some of the former stars have also been considered by Hardorp (1982) to have UV spectral features very similar to the solar ones.

3. Photometric similarity index

The two-dimensional 2σ $((B - V)^{\text{Tycho}}, M_{V_\odot}^{\text{Tycho}})$ box would automatically select solar twins were it not for the metallicity dimension, since surface gravity effects are negligible in the narrow color-magnitude interval involved here. Stars selected by means of color have a dispersion in T_{eff} corresponding to a dispersion in $[\text{Fe}/\text{H}]$. We use throughout the notation $[A/B] = \log N(A)/N(B)_{\text{star}} - \log N(A)/N(B)_{\text{Sun}}$, where N denotes the number abundance of a given element. Thus, a metal-rich star cooler than the Sun may mimic the solar colors, as may a star hotter than the Sun but metal-richer. To narrow down further the candidate list to be observed spectroscopically, we defined a color-similarity index S_C with respect to the Sun:

$$S_C = \alpha \sum_{C_i} \left\{ \frac{(C_i^\star - C_i^\odot)^2}{(\bar{\sigma}_{C_i})^2} \right\} \quad (1)$$

where C_i represents the color indices $(B - V)$, $(B - V)^{\text{Tycho}}$, $(b - y)$, and m_1 , and α is an arbitrary normalization constant. The last color is essentially a photometric metallicity dimension, while the three previous colors are independent measurements of the stellar Paschen continuum. This index then simultaneously reflects the gradient of the Paschen continuum and the strength of metal lines. Attempts to employ the β and $(V - K)$ colors in the definition of the index had to be abandoned owing to the large incompleteness of such data for the program stars. The index S_C expresses a simple sum of quadratic differences with respect to the adopted solar colors, weighted by the average error of each color. The average color errors for the $V^{\text{Tycho}} \leq 8.0$ stars are

$$\langle \sigma \rangle (B - V)^{\text{Johnson}} = 0.009$$

$$\langle \sigma \rangle (B - V)^{\text{Tycho}} = 0.013$$

$$\langle \sigma \rangle (b - y) = 0.003$$

$$\langle \sigma \rangle (m_1) = 0.005.$$

The $(B - V)^{\text{Johnson}}$ and $(B - V)^{\text{Tycho}}$ errors were directly obtained from the Hipparcos catalog, and the $(b - y)$ and m_1 errors are given by Olsen (1983, 1993, 1994a, 1994b) for each object. For the 106 stars within $8.0 < V^{\text{Tycho}} < 9.0$, *uvby* photometry is only available for 68 stars. The corresponding average color errors for the fainter targets are

$$\langle \sigma \rangle (B - V)^{\text{Johnson}} = 0.013$$

$$\langle \sigma \rangle (B - V)^{\text{Tycho}} = 0.020$$

$$\langle \sigma \rangle (b - y) = 0.003$$

$$\langle \sigma \rangle (m_1) = 0.005.$$

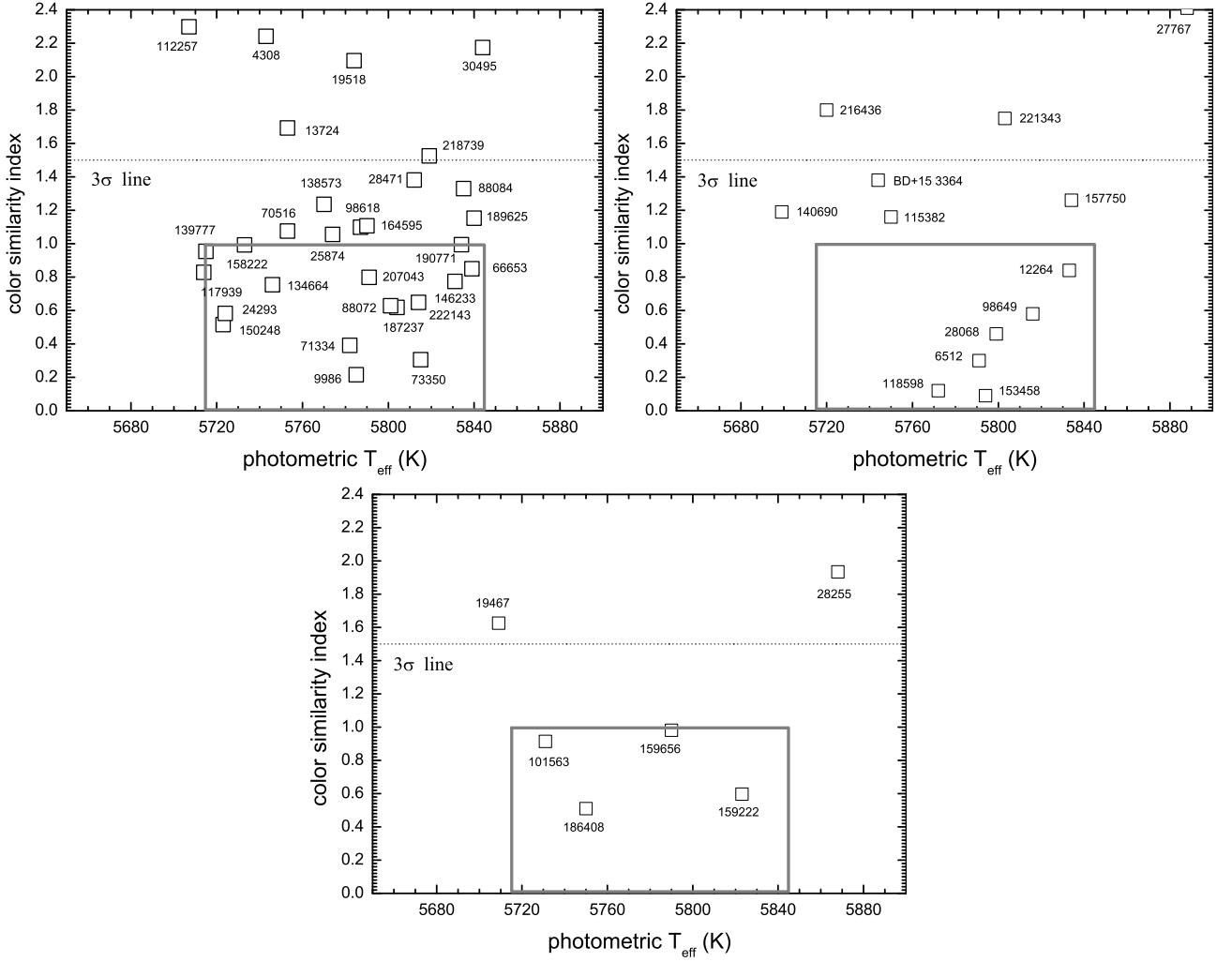


Fig. 2. *Left.* The color similarity index S_C plotted versus the photometric T_{eff} for the 52 stars with $V_{\text{Tycho}} \leq 8.0$. The box contains, in the S_C axis, stars with $S_C \leq 1.00$ within 2σ of the solar one (defined as zero) in the ordinate. The width of the box is set by the $\sigma(T_{\text{eff}}^{\text{phot}}) = 65$ K uncertainty in the photometric T_{eff} . The dotted horizontal line defines the 3σ limit in S_C . Stars are identified by HD numbers. *Right.* The same as the left panel, but for the $8.0 < V_{\text{Tycho}} \leq 9.0$ stars, only those observed spectroscopically. *Below.* Same as above for stars selected by their UVB similarity to the Sun, presence in the lists of Hardorp (1982), or both.

Olsen (1993) discusses systematic discrepancies between the photometry of southern stars (which he calls the "F" catalog of Olsen 1983) and northern stars (Olsen 1993, 1994a,b, the "G" catalog), providing transformations for the homogenization of the photometry. We employed these transformations to convert all the $(b - y)$ and m_1 indices to the "F" catalog of Olsen (1983), since more than half of our prime targets, the $V_{\text{Tycho}} \leq 8.0$ stars, have their photometry in this catalog. Since the color similarity index will be an important tool in the forthcoming discussion, it is very important that the reader keeps in mind that all the Strömgren photometry discussed here is compatible with the catalog of Olsen (1983).

The color-similarity index was computed for the sample taking the different color errors for the $V_{\text{Tycho}} \leq 8.0$ and $8.0 < V_{\text{Tycho}} \leq 9.0$ stars into account. The solar colors obviously correspond to an index $S_C = 0.00$, and the α constant was adjusted in each case so that a 2σ uncertainty in S_C was equal to unity. This was obtained by inserting the solar color themselves into the index equation, added by twice their corresponding errors.

In Fig 2 the color similarity index for the $V_{\text{Tycho}} \leq 8.0$ stars with $S_C \leq 2.4$ is shown. The stars located inside the 2σ box are the best candidates, in principle, since they have the Tycho absolute magnitude and color compatible with the solar ones within a formal 2σ limit. A similar diagram was obtained for the $8.0 < V_{\text{Tycho}} \leq 9.0$ stars. The number of stars within the 2σ boxes for each case was 16 for the brighter and 28 for the fainter candidates. As an initial estimation of the atmospheric parameters, the m_1 -[Fe/H] calibration of McNamara & Powell (1985), along with the photometric T_{eff} calibrations for $(B - V)$, $(B - V)^{\text{Tycho}}$ and $(b - y)$ detailed in the Appendix, were used to obtain photometric T_{eff} and [Fe/H] parameters. Though superseded by recent works, the relation of McNamara & Powell (1985) provides a simple linear m_1 -[Fe/H] relationship for solar-type stars, which is very accurate in a narrow interval around the Sun and well linked to the Hyades iron abundance [Fe/H] = +0.12 (Paulson et al. 2003; Cayrel et al. 1985). These photometrically derived atmospheric parameters are plotted in Fig 3 for all the sample stars for which *uvby* photometry is available and the S_C defined. The solar colors, once entered into this set of

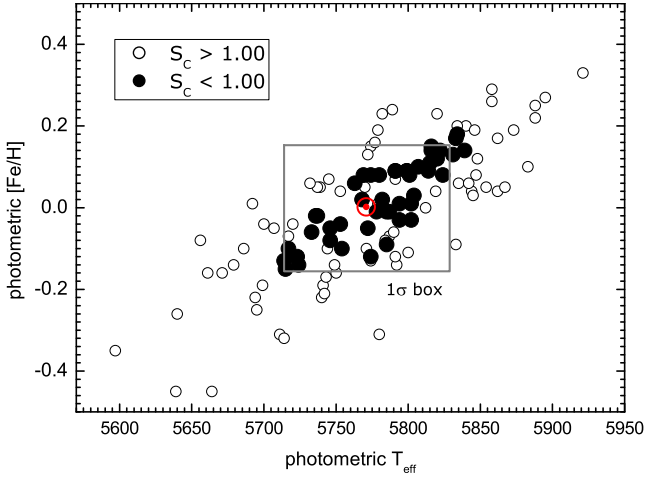


Fig. 3. Photometric T_{eff} s and $[\text{Fe}/\text{H}]$ s, separated by the color similarity index S_c . The gray box limits the 1σ errors in the photometric T_{eff} s and $[\text{Fe}/\text{H}]$ s, and is centered on the solar parameters (the Sun is identified by its usual symbol). Black circles are those stars within a 2σ color similarity with the Sun.

calibrations, yields $T_{\text{eff} \odot} = 5774 \text{ K}$ and $[\text{Fe}/\text{H}] = -0.03$, assuring us that no significant systematic error is incurred by the procedure. The photometrically derived $[\text{Fe}/\text{H}]$ s, when compared with the final spectroscopic ones (see section 4), define a linear regression with a low correlation coefficient of $R = 0.32$, but no systematic deviation from the identity line. Under the reasonable hypothesis of statistical independence, the total dispersion of the regression, $\sigma = 0.16 \text{ dex}$, yields $\sigma([\text{Fe}/\text{H}]^{\text{phot}}) = 0.14 \text{ dex}$, when the errors of the spectroscopically determined $[\text{Fe}/\text{H}]$ are taken into account (section 4). When entered into the T_{eff} calibrations, this uncertainty in $[\text{Fe}/\text{H}]^{\text{phot}}$, along with the already determined errors in the colors, fixes the uncertainty of the photometrically derived T_{eff} s. We obtained $\sigma(T_{\text{eff}}^{\text{phot}}) = 65 \text{ K}$, a value that surpasses the expected internal dispersion of T_{eff} s derived from the $(B - V)$, $(B - V)^{\text{Tycho}}$ and $(b - y)$ calibrations, as discussed in the Appendix. This can be explained by the larger errors in colors and $[\text{Fe}/\text{H}]$ of the sample stars, as compared with the much brighter stars used to obtain the photometric calibrations. For stars not observed spectroscopically (section 4), these are our final determination of the atmospheric parameters and absolute magnitudes. For all the sample, the colors, color similarity indices, along with the photometrically derived T_{eff} , $[\text{Fe}/\text{H}]$, and absolute magnitudes (in the V^{Tycho} band) are shown in Tables 1, 2, and 3.

In Fig 3, those stars with a 2σ color similarity with the Sun are clearly contained within the box that defines atmospheric parameters T_{eff} and $[\text{Fe}/\text{H}]$ within 65 K and 0.14 dex, respectively, from the solar values. It will be shown below that the color similarity index is indeed very efficient in selecting stars which not only are photometrically similar to the Sun, but also possess atmospheric parameters contained within a narrow interval of the solar ones, as determined from a spectroscopic model atmospheres analysis. This approach allows a fast and convenient photometric selection of stars resembling any desired set of colors and atmospheric parameters, expeditiously diminishing the necessity of spectroscopic follow-up, provided that the colors are sufficiently accurate.

4. Observations and reductions

4.1. OPD optical spectra

Spectroscopic observations were performed with the coude spectrograph, coupled to the 1.60m telescope of Observatório do Pico dos Dias (OPD, Brazópolis, Brazil), operated by Laboratório Nacional de Astrofísica (LNA/CNPq), in a series of runs from 1998 to 2002. Spectra were obtained for 47 stars in 2 spectral ranges, $\sim 150 \text{ \AA}$ wide, centered at $\lambda 6145$ and $\lambda 6563$ ($\text{H}\alpha$). The nominal resolution was $R = 20\,000$ per resolution element, and the S/N ranged from 50 to 440, with an average value of 160. Four stars were only observed in the $\lambda 6145$ range, and one star only in the $\lambda 6563$ range. Three objects, HD 73350, HD 146233 (18 Sco), and HD 189625 were observed in separate epochs and reduced and analyzed separately as a procedure control. As proxies of the solar flux spectrum, the Galilean satellites Europa, Ganymede, and Callisto were observed in both spectral ranges; Io was only observed in the $\lambda 6563$ range.

Data reduction was carried out by the standard procedure using IRAF¹. Bias and flat-field corrections were performed, background and scattered light were subtracted, and the one-dimensional spectra were extracted. The pixel-to-wavelength calibration was obtained from the stellar spectra themselves, by selecting isolated spectral lines in the object spectra and checking for the absence of blends, the main screen for blends being the Solar Flux Atlas (Kurucz et al. 1984) and the Utrecht spectral line compilation (Moore et al. 1966). There followed the Doppler correction of all spectra to a rest reference frame. Continuum normalization was performed by fitting low-order polynomials to line-free regions, and a careful comparison to the solar flux spectrum was carried out to ensure a high degree of homogeneity in the procedure. The equivalent widths (hereafter W_{λ} s) of a set of unblended, weak, or moderately strong lines of Fe I and Fe II were measured by Gaussian fitting in all stars, totalling 15 and 2 lines, respectively, for the best exposed spectra. Sample OPD spectra are shown in Fig. 4.

4.2. ESO/FEROS spectra

The FEROS spectrograph (Kaufer et al. 1999) was used to obtain data for 17 stars, in three runs from 2000 to 2002. Six stars are common between the FEROS and OPD data sets, as a homogeneity test: HD 19518, HD 73350, HD 98649, HD 105901, HD 115382, and HD 146233. A FEROS spectrum of Ganymede was also secured. The standard FEROS pipeline of spectral reduction was used, and the spectra were degraded to the same resolution of the OPD spectra, and clipped to the same wavelength range. The blaze curvature, unfortunately, precluded our use of the $\text{H}\alpha$ profile of the FEROS data. The S/N of the degraded FEROS spectra ranged from 100 to 700, the average value being 400. After this procedure, the data reduction followed exactly the same steps as the OPD data.

4.3. ESO UV spectra

The cassegrain Boller & Chivens spectrograph of the ESO 1.52m telescope was used in two runs, in 1997 and 1998, to acquire low-resolution spectra for 37 stars, plus four proxies of the so-

¹ *Image Reduction and Analysis Facility* (IRAF) is distributed by the National Optical Astronomical Observatories (NOAO), which is operated by the Association of Universities for Research in Astronomy (AURA), Inc., under contract to the National Science Foundation (NSF).

Table 1. Photometric and spectroscopic data for the program stars with $V_T \leq 8.0$. The second to sixth columns provide V^{Tycho} , $(B - V)^{\text{Johnson}}$, $(B - V)^{\text{Tycho}}$, $(b - y)$, and m_1 , respectively. The seventh column gives the photometric similarity index with respect to the solar colors (see text). Columns 8 and 9 list the photometrically derived effective temperature T_{eff} and metallicity. Columns 10 and 11 list the visual absolute magnitude from the Tycho V_T band and its corresponding uncertainty, respectively. Columns 12, 13, and 14 list the S/N ratios of the spectroscopic observations as follows: $\lambda 6145$ and $\lambda 6563$ ranges from the OPD coude spectrograph; FEROS spectrograph. The last column merely notes if low-resolution UV spectra from the Boller-Chivens Cassegrain spectrograph of the ESO 1.52m telescope have been obtained.

HD	V^{Tycho}	$(B - V)^{\text{Johnson}}$	$(B - V)^{\text{Tycho}}$	$(b - y)$	m_1	S_C	$T_{\text{eff}}^{\text{phot}}$	$[\text{Fe}/\text{H}]_{\text{phot}}$	M_V^{Tycho}	$\sigma(M_V^{\text{Tycho}})$	$\lambda 6145$	$\lambda 6563$	FEROS	UV
1835	6.5	0.659	0.758	0.422	0.225	4.03	5686	-0.10	4.90	0.05	—	—	—	
4308	6.6	0.655	0.723	0.402	0.198	2.24	5743	-0.17	4.93	0.04	280	180	—	√
9986	6.8	0.648	0.720	0.408	0.217	0.22	5785	-0.01	4.79	0.06	—	—	220	
11131	6.8	0.654	0.711	0.403	0.188	4.85	5711	-0.31	4.98	0.23	—	—	—	
13724	8.0	0.667	0.746	0.414	0.228	1.69	5753	+0.04	4.78	0.10	70	140	—	√
18757	6.7	0.634	0.729	0.417	0.191	5.40	5639	-0.45	4.92	0.05	—	—	—	
19518	7.9	0.642	0.731	0.399	0.203	2.10	5784	-0.08	4.84	0.11	120	—	450	√
24293	7.9	0.658	0.727	0.412	0.211	0.58	5724	-0.14	4.79	0.10	60	90	—	√
25680	6.0	0.620	0.720	0.397	0.212	3.45	5854	+0.05	4.85	0.05	—	—	—	
25874	6.8	0.667	0.747	0.410	0.227	1.06	5774	+0.08	4.77	0.04	170	170	—	
28471	8.0	0.650	0.717	0.399	0.210	1.38	5812	+0.00	4.79	0.08	—	—	—	
28701	7.9	0.650	0.710	0.402	0.186	5.64	5714	-0.32	4.76	0.08	—	—	—	
28821	7.7	0.683	0.747	0.422	0.205	5.31	5597	-0.35	4.85	0.10	80	170	—	√
30495	5.6	0.632	0.710	0.399	0.213	2.18	5844	+0.04	4.94	0.04	260	380	—	
32963	7.7	0.664	0.743	0.403	0.237	2.46	5858	+0.29	4.92	0.10	—	—	410	√
35041	7.7	0.636	0.731	0.395	0.213	2.58	5847	+0.08	4.89	0.10	—	—	250	√
37773	7.8	0.692	0.746	0.429	0.236	10.90	5656	-0.08	4.90	0.11	—	—	610	√
64184	7.6	0.675	0.755	0.420	0.218	3.45	5661	-0.16	4.95	0.07	—	—	—	
66653	7.6	0.655	0.726	0.400	0.222	0.85	5839	+0.14	4.80	0.06	130	—	560	√
68168	7.4	0.667	0.729	0.419	0.224	2.52	5717	-0.07	4.79	0.09	—	—	630	√
70516	7.8	0.652	0.725	0.415	0.222	1.08	5753	-0.04	4.93	0.19	—	—	—	
71334	7.9	0.643	0.746	0.408	0.220	0.39	5782	+0.02	4.92	0.09	—	220	660	√
73350	6.8	0.655	0.731	0.405	0.224	0.31	5815	+0.11	4.95	0.07	180	210	700	
76151	6.1	0.661	0.752	0.410	0.239	2.93	5820	+0.23	4.91	0.04	—	—	—	
77006	8.0	0.651	0.707	0.384	0.202	9.07	5867	+0.05	4.82	0.11	—	—	—	
86226	8.0	0.647	0.719	0.381	0.204	10.48	5883	+0.10	4.85	0.10	—	—	—	
88072	7.6	0.647	0.753	0.404	0.221	0.63	5801	+0.08	4.74	0.10	—	—	250	
88084	7.6	0.649	0.712	0.399	0.215	1.33	5835	+0.06	4.87	0.08	—	—	—	
98618	7.7	0.642	0.713	0.404	0.208	1.10	5787	-0.07	4.78	0.09	—	—	—	
108575	8.0	0.68	0.745	0.417	0.234	3.37	5745	+0.07	4.90	0.34	—	—	—	
112257	7.9	0.665	0.758	0.417	0.223	2.30	5707	-0.05	4.76	0.11	—	—	—	
114174	6.9	0.667	0.757	0.418	0.233	3.72	5737	+0.05	4.76	0.07	—	—	—	
117939	7.4	0.669	0.738	0.409	0.208	0.83	5714	-0.13	4.96	0.07	140	120	—	
134664	7.8	0.662	0.739	0.404	0.207	0.76	5746	-0.08	4.83	0.12	100	180	—	
138573	7.3	0.656	0.745	0.413	0.228	1.24	5770	+0.05	4.85	0.07	130	120	—	
139777	6.7	0.665	0.723	0.413	0.211	0.95	5715	-0.15	4.94	0.04	—	—	—	
142072	7.9	0.670	0.749	0.420	0.210	3.21	5640	-0.26	4.83	0.11	120	170	—	
145825	6.6	0.646	0.727	0.395	0.228	2.74	5895	+0.27	4.93	0.06	180	230	—	
146233	5.6	0.652	0.736	0.400	0.221	0.78	5831	+0.13	4.83	0.04	340	230	380	√
150248	7.1	0.653	0.740	0.412	0.212	0.52	5723	-0.12	4.83	0.08	180	200	—	
155114	7.6	0.637	0.720	0.396	0.197	4.27	5791	-0.12	4.85	0.09	140	120	—	√
158222	7.9	0.667	0.727	0.414	0.219	0.99	5733	-0.06	4.83	0.08	—	—	—	
164595	7.1	0.635	0.722	0.404	0.209	1.11	5790	-0.06	4.84	0.06	190	160	—	
187237	7.0	0.660	0.718	0.402	0.215	0.62	5804	+0.03	4.88	0.05	—	—	100	
189567	6.1	0.648	0.718	0.399	0.199	2.76	5774	-0.13	4.90	0.04	—	—	—	
189625	7.4	0.654	0.729	0.406	0.232	1.15	5840	+0.20	4.74	0.09	150	110	—	√
190771	6.3	0.654	0.732	0.406	0.231	1.00	5834	+0.18	4.89	0.04	290	150	—	√
202628	6.8	0.637	0.710	0.396	0.210	2.83	5845	+0.03	4.95	0.06	—	—	—	
207043	7.7	0.660	0.737	0.410	0.228	0.80	5791	+0.09	5.01	0.08	130	160	—	
214385	8.0	0.640	0.723	0.403	0.195	3.03	5740	-0.22	4.97	0.11	120	—	—	√
218739	7.2	0.658	0.716	0.398	0.212	1.53	5819	+0.04	4.86	0.16	—	—	—	
222143	6.7	0.665	0.724	0.402	0.220	0.65	5814	+0.09	4.85	0.05	—	—	—	

lar flux spectrum: Vesta, Ganymede, Callisto and Io. The useful spectral range was $\lambda\lambda 3600\text{--}4600$, and the nominal spectral resolution was $R = 2\,000$. The exposure times were set to obtain S/N around 100, and only a few cases fell short of this goal. All spectra were reduced in a standard way and wavelength-calibrated. Offsets in the wavelength calibration were corrected by shifting all spectra to agree with the wavelength scale of the Ganymede spectrum. Spectra were then degraded to a resolution of $R = 800$, and the resulting S/N is better than 200 in all cases. The spec-

tra were normalized and ratioed to the Ganymede spectrum. We estimated errors in the flux spectra remaining from errors in the wavelength calibration as no larger than 1%. Errors due to the normalization procedure were estimated by comparing the ratio spectra of Vesta, Callisto, and Io to that of Ganymede, and attributing all fluctuations to random noise in the normalization: an average value of $1\sigma = 1.8\%$ results. The Ganymede spectrum was chosen as the preferred reference solar proxy. A similar exercise with the spectra of five stars very similar to the Sun in their

Table 2. The same as Table 1 for the 70 program stars with $8.0 < V_T \leq 9.0$ and available *uvby* photometry. Owing to a management error, we also observed two stars not inside the Hipparcos 2σ box, HD 140690, and HD 216436, plus one star inside the box, but without *uvby* photometry, HD 8291: the [Fe/H] of the latter was arbitrarily set to solar.

HD	V^{Tycho}	$(B - V)^{\text{Johnson}}$	$(B - V)^{\text{Tycho}}$	$(b - y)$	m_1	S_C	$T_{\text{eff}}^{\text{phot}}$	[Fe/H] _{phot}	M_V^{Tycho}	$\sigma (M_V^{\text{Tycho}})$	$\lambda 6145$	$\lambda 6563$	FEROS	UV
3810	8.8	0.638	0.713	0.396	0.196	4.19	5792	-0.14	4.96	0.17	—	—	—	
6512	8.2	0.656	0.746	0.407	0.224	0.30	5791	+0.09	4.81	0.12	—	—	—	✓
8291	8.7	0.638	0.736	—	—	—	5794	+0.00	4.83	0.17	90	80	—	✓
7678	8.3	0.646	0.718	0.399	0.223	1.18	5862	+0.17	4.91	0.11	—	—	—	
12264	8.1	0.660	0.736	0.401	0.225	0.84	5833	+0.17	4.85	0.13	80	110	—	✓
15507	8.7	0.670	0.749	0.423	0.240	6.46	5732	+0.06	4.87	0.14	—	—	—	
15632	8.1	0.666	0.749	0.413	0.222	0.81	5736	-0.02	4.99	0.12	—	—	—	
17439	8.7	0.668	0.747	0.416	0.237	3.33	5772	+0.13	5.00	0.12	—	—	—	
19617	8.8	0.682	0.746	0.430	0.245	11.89	5692	+0.01	4.99	0.19	—	—	—	
21543	8.3	0.619	0.713	0.388	0.176	14.44	5780	-0.31	5.00	0.14	—	—	—	
26736	8.1	0.657	0.709	0.407	0.232	1.31	5846	+0.19	4.83	0.13	—	—	—	
26767	8.1	0.640	0.724	0.395	0.224	2.41	5888	+0.22	4.88	0.17	—	—	—	✓
27857	8.1	0.657	0.715	0.402	0.213	0.53	5802	+0.01	4.81	0.13	—	—	—	
28068	8.1	0.651	0.734	0.409	0.226	0.46	5799	+0.09	4.80	0.16	—	—	—	✓
31130	8.9	0.655	0.730	0.407	0.225	0.32	5807	+0.10	4.97	0.14	—	—	—	
34599	8.4	0.660	0.737	0.405	0.222	0.21	5799	+0.09	5.00	0.10	—	—	—	
35769	8.7	0.689	0.755	0.412	0.241	4.28	5789	+0.24	4.98	0.19	—	—	—	
36152	8.3	0.657	0.752	0.408	0.224	0.37	5780	+0.08	4.99	0.13	—	—	—	
41708	8.1	0.626	0.712	0.393	0.208	3.84	5862	+0.04	4.85	0.13	—	—	—	
43180	8.4	0.658	0.734	0.390	0.212	4.16	5848	+0.12	4.87	0.10	—	—	—	✓
45346	8.7	0.661	0.738	0.399	0.219	0.95	5820	+0.12	4.78	0.12	—	—	—	
75288	8.6	0.673	0.754	0.417	0.243	5.17	5779	+0.19	4.75	0.13	—	—	—	
76332	8.6	0.620	0.735	0.405	0.213	0.99	5802	-0.03	4.99	0.17	—	—	—	
78130	8.8	0.674	0.755	0.413	0.236	2.75	5777	+0.16	4.85	0.16	—	—	—	
78660	8.4	0.665	0.724	0.406	0.227	0.62	5816	+0.14	4.91	0.14	—	—	—	
81700	8.6	0.650	0.733	0.402	0.211	0.53	5787	-0.01	4.89	0.11	—	—	—	
90322	8.8	0.641	0.711	0.404	0.207	0.90	5785	-0.09	4.98	0.18	—	—	—	
90333	8.4	0.676	0.738	0.404	0.216	0.49	5768	+0.02	4.91	0.12	—	—	—	
93215	8.1	0.670	0.758	0.413	0.235	2.50	5774	+0.15	4.75	0.12	—	—	—	
98649	8.1	0.658	0.741	0.405	0.227	0.58	5816	+0.15	4.91	0.11	120	140	420	
105901	8.3	0.626	0.728	0.395	0.197	4.58	5800	-0.11	4.78	0.13	110	250	240	
110668	8.3	0.672	0.752	0.408	0.223	0.54	5763	+0.06	4.74	0.15	—	—	—	
110869	8.1	0.662	0.748	0.414	0.223	0.97	5737	-0.02	4.81	0.10	—	—	—	
110979	8.1	0.654	0.751	0.408	0.214	0.16	5746	-0.05	4.77	0.13	—	—	—	
111069	8.7	0.630	0.720	0.399	0.236	3.17	5921	+0.33	4.87	0.19	—	—	—	
111938	8.5	0.632	0.713	0.407	0.207	0.98	5774	-0.12	4.91	0.13	—	—	—	
115231	8.5	0.667	0.756	0.419	0.217	2.29	5671	-0.16	4.86	0.15	—	—	—	
115382	8.5	0.630	0.731	0.408	0.205	1.16	5750	-0.16	4.80	0.17	140	110	330	
118598	8.3	0.652	0.721	0.407	0.213	0.12	5772	-0.05	4.84	0.13	130	130	—	
121205	9.0	0.675	0.756	0.395	0.212	2.61	5791	+0.07	4.87	0.19	—	—	—	
123682	8.4	0.690	0.756	0.410	0.209	1.56	5679	-0.14	4.93	0.14	—	—	—	
126267	8.9	0.680	0.743	0.421	0.229	3.97	5700	-0.04	4.83	0.16	—	—	—	
129920	8.3	0.659	0.711	0.409	0.211	0.40	5754	-0.10	4.90	0.09	—	—	—	
133430	8.6	0.669	0.729	0.406	0.196	2.39	5695	-0.25	4.99	0.11	—	—	—	
134702	8.4	0.645	0.716	0.405	0.213	0.28	5794	-0.03	4.91	0.16	—	—	—	
140690	8.6	0.659	0.729	0.415	0.210	1.19	5699	-0.19	4.74	0.12	110	160	—	✓
143337	8.1	0.639	0.729	0.406	0.180	7.03	5664	-0.45	4.80	0.15	80	180	—	✓
153458	8.1	0.652	0.723	0.405	0.216	0.09	5794	+0.01	4.85	0.12	140	100	—	
154221	8.7	0.640	0.710	0.402	0.232	1.78	5888	+0.25	4.77	0.21	—	—	—	
155968	8.5	0.687	0.752	0.416	0.245	5.96	5782	+0.23	4.86	0.15	—	—	—	
157750	8.1	0.670	0.721	0.405	0.231	1.26	5834	+0.20	4.88	0.16	110	120	—	✓
158415	8.4	0.681	0.744	0.406	0.222	0.71	5769	+0.08	4.85	0.09	—	—	—	
163441	8.5	0.685	0.750	0.402	0.217	1.14	5767	+0.06	4.76	0.15	—	—	—	
163859	8.6	0.660	0.753	0.411	0.213	0.45	5717	-0.10	4.92	0.10	—	—	—	
BD+15 3364	8.7	0.647	0.733	0.411	0.213	1.38	5744	-0.10	4.83	0.17	110	150	—	
171226	8.9	0.648	0.720	0.420	0.233	3.70	5767	+0.02	4.97	0.19	—	—	—	
181199	8.2	0.656	0.752	0.407	0.199	1.73	5694	-0.22	4.78	0.26	—	—	—	
183579	8.8	0.653	0.727	0.399	0.216	0.90	5824	+0.08	4.91	0.17	—	—	—	
188298	8.5	0.657	0.718	0.408	0.229	0.81	5822	+0.14	4.92	0.17	—	—	—	
191487	8.6	0.654	0.729	0.390	0.217	4.01	5873	+0.19	4.79	0.16	100	130	—	✓
200633	8.4	0.639	0.728	0.406	0.201	1.46	5741	-0.19	4.76	0.16	—	—	—	
202072	8.2	0.665	0.725	0.399	0.198	2.80	5749	-0.14	4.78	0.13	90	100	—	✓
204627	8.7	0.610	0.727	0.391	0.196	7.20	5833	-0.09	4.98	0.16	—	—	—	
206772	8.4	0.653	0.709	0.394	0.210	2.77	5842	+0.06	4.79	0.10	—	—	—	
209262	8.1	0.687	0.752	0.411	0.225	1.46	5739	+0.05	4.77	0.13	—	—	—	
211786	8.1	0.666	0.726	0.394	0.197	4.46	5771	-0.10	4.96	0.11	130	100	—	✓
214635	8.7	0.672	0.733	0.400	0.211	1.10	5779	+0.01	4.91	0.16	—	—	—	
215942	8.1	0.664	0.723	0.404	0.213	0.31	5778	-0.01	4.80	0.11	—	—	—	
216436	8.7	0.676	0.740	0.415	0.222	1.80	5720	-0.04	4.74	0.11	70	100	—	✓
221343	8.4	0.657	0.733	0.404	0.235	1.75	5858	+0.26	4.84	0.14	50	40	—	✓
BD+40 5199	8.2	0.652	0.731	0.397	0.191	4.77	5742	-0.21	5.01	0.10	—	—	—	

Table 3. The same as Table 1 for the Galilean satellites and Vesta (taken as proxies of the solar flux spectrum) plus stars selected in the Bright Star Catalogue (Hoffleit & Jaschek 1991; Hoffleit 1991) to have both their $(B - V)$ and $(U - B)$ colors similar to the solar ones.

HD	V^{Tycho}	$(B - V)^{\text{Johnson}}$	$(B - V)^{\text{Tycho}}$	$(b - y)$	m_1	S_C	$T_{\text{eff}}^{\text{phot}}$	$[\text{Fe}/\text{H}]_{\text{phot}}$	M_V^{Tycho}	$\sigma (M_V^{\text{Tycho}})$	$\lambda 6145$	$\lambda 6563$	FEROS	UV
Ganymede	—	—	—	—	—	—	—	—	—	—	250	330	510	✓
Callisto	—	—	—	—	—	—	—	—	—	—	440	230	—	✓
Europa	—	—	—	—	—	—	—	—	—	—	390	290	—	—
Io	—	—	—	—	—	—	—	—	—	—	—	250	—	✓
Vesta	—	—	—	—	—	—	—	—	—	—	—	—	—	✓
9562	5.8	0.639	0.709	0.389	0.221	5.43	5919	+0.24	3.47	0.05	—	—	—	✓
16141	6.9	0.670	0.751	0.424	0.211	4.87	5614	−0.31	4.12	0.11	—	—	—	✓
19467	7.0	0.645	0.734	0.409	0.200	1.63	5709	−0.23	4.56	0.06	—	—	—	✓
28255	6.0	0.659	0.730	0.397	0.227	1.94	5868	+0.24	3.81	0.08	—	—	—	✓
94340	7.1	0.645	0.702	0.398	0.204	2.93	5811	−0.05	4.03	0.10	210	250	—	—
101563	6.5	0.651	0.719	0.410	0.206	0.91	5731	−0.17	3.41	0.08	—	—	210	—
105590	6.8	0.666	0.753	0.404	0.233	4.20	5884	+0.34	4.65	0.63	170	180	—	—
111398	7.2	0.660	0.724	0.420	0.223	2.65	5717	−0.10	4.37	0.09	—	—	440	—
119550	7.0	0.631	0.698	0.411	0.202	3.23	5744	−0.23	3.09	0.14	170	160	—	—
159222	6.6	0.639	0.722	0.404	0.219	0.60	5823	+0.06	4.72	0.04	240	200	—	✓
159656	7.2	0.641	0.711	0.405	0.210	0.98	5790	−0.06	4.61	0.09	130	170	—	✓
186408	6.0	0.643	0.728	0.410	0.211	0.51	5750	−0.11	4.36	0.04	180	—	—	—
221627	6.9	0.666	0.739	0.421	0.204	3.82	5622	−0.35	3.47	0.10	250	160	—	✓

UV spectral features yielded $1\sigma = 1.6\%$. We estimate that $1\sigma \sim 2\%$ is a conservative estimate of the flux ratio uncertainty of the spectral features in the UV spectra, between $\lambda 3700$ and $\lambda 4500$. Shortward of $\lambda 3700$ the lower S/N and very strong blending introduce a larger uncertainty in the ratio spectra of strong-lined stars. Samples of the unratied and ratied spectra are shown in Fig. 5.

The main goal for the UV data is to verify to what extent, in the spectra of solar analogs, the strength of the CN and CH bands, both very sensitive to the stellar atmospheric parameters, remain similar to the solar ones. Also, the flux ratio at the core of the Ca II H and K lines, at $\lambda\lambda$ 3968 and 3934, is very sensitive to the stellar chromospheric filling, and therefore to age, at least within ~ 2 Gyr of the ZAMS (Pace & Pasquini 2004).

There are 24 stars in our sample with $V^{\text{Tycho}} \leq 8.0$, color similarity index $S_C < 1.50$ (corresponding to a 3σ similarity) and accessible from the southern hemisphere. All of them were observed at either the OPD or FEROS/ESO, excepting HD 28471 and HD 88084. Actually, only four northern objects matching the above criteria, HD 70516, HD 98618, HD 139777, and HD 158222 are inaccessible from either the OPD or FEROS locations. In Tables 1, 2, and 3, the available spectral data for each star is indicated. Quality checks were performed on the measured W_λ s following the same procedure as discussed in detail by Porto de Mello et al. (2008). Saturated lines were eliminated by a 2σ clipping on the relation of reduced width W_λ/λ with line depth, and no lines were measured beyond the linearity limit. Also, no trend is expected in the relation of the line full-width-half-maximum and reduced width, since the line widths are defined by the instrumental profile. The measured W_λ s were corrected to bring them onto a system compatible with the Voigt-fitted W_λ s of Meylan et al. (1993). This correction is +5.0% for the OPD and +6.0% for the FEROS/ESO W_λ s. In Table 4 we list the Fe I and Fe II lines used with the corresponding excitation potentials and gf -values derived. The W_λ s measurements of all analyzed stars are available upon request.

Table 4. The Fe I and Fe II transitions used in the spectroscopic analysis. The first two columns are self-explanatory; the third and fourth columns are, respectively, the (raw) W_λ s measured off the OPD and FEROS Ganymede spectra (both in mÅ); the fifth column is the lower excitation potential (in eV); and the last column is the log gf derived from the OPD spectra.

Wavelength (Å)	Species	W_λ (OPD)	W_λ (FEROS)	χ (eV)	log gf
6078.499	Fe I	85.1	83.0	4.79	−0.274
6079.016	Fe I	51.8	51.0	4.65	−0.942
6084.105	Fe II	25.7	25.1	3.20	−3.717
6089.574	Fe I	40.9	41.3	5.02	−0.811
6093.649	Fe I	36.8	37.6	4.61	−1.263
6096.671	Fe I	44.9	41.1	3.98	−1.692
6102.183	Fe I	92.2	86.9	4.83	−0.144
6149.249	Fe II	38.4	37.5	3.89	−2.752
6151.623	Fe I	52.1	52.8	2.18	−3.292
6157.733	Fe I	69.4	66.1	4.07	−1.143
6159.382	Fe I	14.6	14.0	4.61	−1.827
6165.363	Fe I	47.6	48.1	4.14	−1.492
6173.341	Fe I	72.0	71.8	2.22	−2.835
6185.704	Fe I	20.7	17.2	5.65	−0.695
6187.995	Fe I	49.4	49.9	3.94	−1.646
6191.571	Fe I	134.1	136.4	2.43	−1.600
6200.321	Fe I	81.2	76.7	2.61	−2.274

5. Results

5.1. Spectroscopic atmospheric parameters

For the determination of the atmospheric parameters T_{eff} , $\log g$ and $[\text{Fe}/\text{H}]$, we employed a strictly differential analysis with the Sun as the standard star. The expectation of this approach is that systematic errors in the measurement of line strengths, the representation of model atmospheres, and the possible presence of non-local thermodynamic equilibrium (NLTE) effects, will be greatly lessened, given the high similarity of all program stars and the Sun. For each spectroscopic data set, at least one point-source solar proxy was observed in a manner identical to that of the stars.

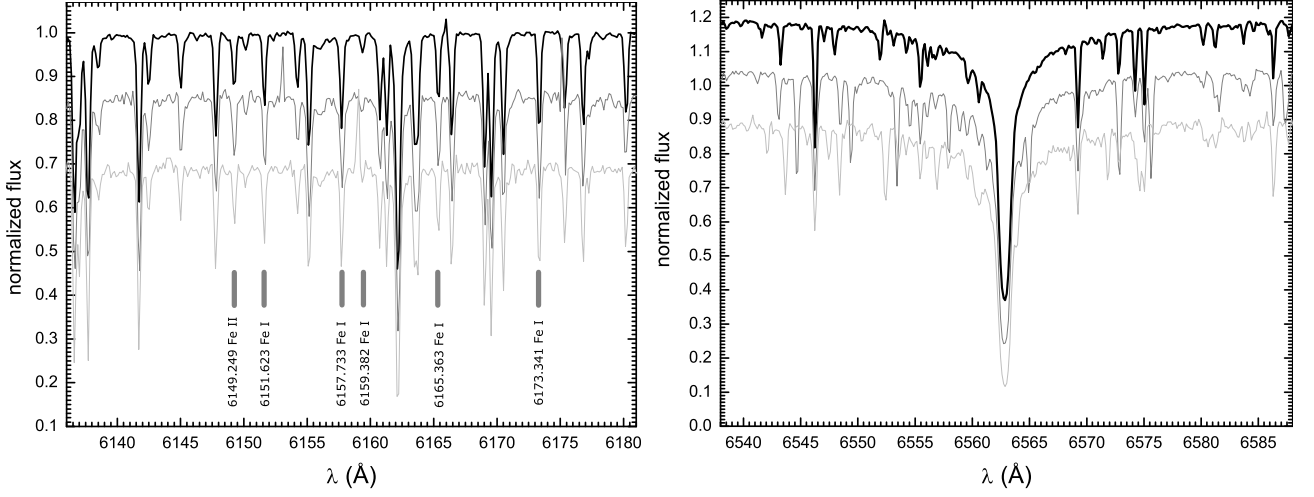


Fig. 4. *Left.* Sample of normalized OPD spectra in the $\lambda 6145$ spectral range. The nominal resolution is $R = 20\,000$, and the spectra S/N, from top to bottom, are 340 (HD 146233), 120 (HD 19518) and 100 (HD 191487). Some of the Fe I and Fe II lines used in this spectral range for deriving atmospheric parameters are marked by the vertical dashes. The spectra are arbitrarily displaced on the vertical axis. *Right.* Sample of normalized OPD spectra in the $\lambda 6563$ spectral range. The nominal resolution is $R = 20\,000$, and the spectra S/N, from top to bottom, are 230 (HD 146233), 200 (HD 159222), and 130 (HD 191487). The spectra are arbitrarily displaced on the vertical axis.

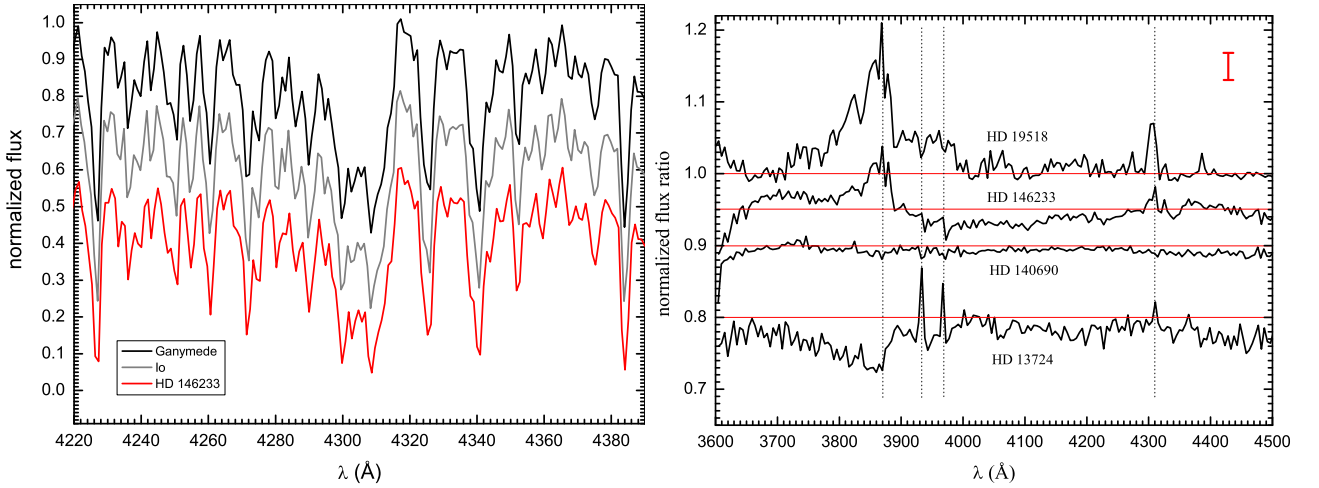


Fig. 5. *Left.* Sample of normalized ESO/UV spectra in the $\lambda\lambda 4220$ -4390 range, around the $\lambda 4310$ CH bandhead. The nominal resolution is $R = 800$, and the spectra are arbitrarily displaced on the vertical axis. *Right.* Sample ratioed ESO/UV spectra, normalized to the solar (Ganymede) spectra, in the $\lambda\lambda 3600$ -4500 range. The spectra are arbitrarily displaced in the vertical axis, and the horizontal red lines mark the unitary flux ratios for each object. The dotted lines are, from left to right, respectively, the approximate central wavelength of the $\lambda 3870$ CN bandhead, the central wavelengths of the K and H Ca II lines, and the approximate central wavelength of the $\lambda 4310$ CH bandhead. The 1σ flux ratio error bar is shown in red.

Solar gf -values were determined for the Fe I and Fe II spectral lines, from solar W_λ s measured off the Ganymede spectra (corrected to the Voigt scale), and an LTE, 1-D, homogeneous and plane-parallel solar model atmosphere from the grid described by Edvardsson et al. (1993). The adopted parameters for the Sun were $T_{\text{eff}} = 5780$ K, surface gravity $\log g = 4.44$, $[\text{Fe}/\text{H}] = +0.00$ and $\xi_t = 1.30 \text{ km s}^{-1}$. The adopted solar absolute abundances (which are inconsequential in a differential analysis) are those of Grevesse & Noels (1993), and gf values were independently generated for the OPD and FEROS data sets.

The atmospheric parameters of the program stars were determined by iterating the photometric T_{eff} (calibrations for which are described in the Appendix) determined from the $(B -$

$V)^{\text{Johnson}}$, $(B - V)^{\text{Tycho}}$, and $(b - y)$ color indices, coupled to the spectroscopic metallicity derived from the Fe I lines. Model atmospheres were interpolated at each step, until the spectroscopic $[\text{Fe}/\text{H}]$ agreed with the model input. Once the photometric T_{eff} are fixed, the $\log g$ was varied until consistency was achieved between the Fe I and Fe II abundances, to a tolerance of 0.01 dex. The microturbulence velocity in all steps was set by the relation of Edvardsson et al. (1993), as a function of T_{eff} and $\log g$. The photometric calibration and set of Fe W_λ s of each star uniquely determines the atmospheric parameter solution.

It is noteworthy that excellent agreement was obtained for the control stars between the atmospheric parameters from two independent determinations based on OPD data, for three stars.

The average differences, respectively, for T_{eff} , $\log g$, and $[\text{Fe}/\text{H}]$ are 13 K, 0.06 dex and 0.03 dex, well within the errors of the analysis. Similarly, for seven stars in common between the OPD and FEROS/ESO data sets, the mean difference in the sense OPD minus FEROS, for T_{eff} , $\log g$ and $[\text{Fe}/\text{H}]$ is +19 K, +0.02 dex and +0.06 dex, respectively, also well within the errors of the analysis. We may thus regard the two data sets as homogeneous, and we show the spectroscopic parameters for all observed stars in Tables 5, 6, and 7. For the control objects, we list the averaged values of all available determinations.

5.2. Effective temperature from the $H\alpha$ profile

Additional effective temperatures were determined for those stars observed in the OPD in the $\lambda 6563$ range by fitting the $H\alpha$ line profiles by Lyra & Porto de Mello (2005), so we refer the reader to this paper for details. For the Galilean satellites, no T_{eff} determination from $H\alpha$ was provided by Lyra & Porto de Mello (2005): for these objects and for some stars also not analyzed by these authors, we determined the $H\alpha$ T_{eff} using exactly the same procedure. The $H\alpha$ profile wings are very sensitive to T_{eff} but barely respond to the other atmospheric parameters. They are particularly insensitive to metallicity (Fuhrmann et al. 1993), and therefore a robust independent check on T_{eff} . The average uncertainty of the T_{eff} ($H\alpha$) determinations is a direct function of the spectral S/N, given the very strong similarity in parameters of all the program stars. This was estimated by the error analysis provided by Lyra & Porto de Mello (2005), and $\sigma(T_{\text{eff}}(H\alpha)) = 50$ K resulted. These T_{eff} s are very closely tied to the solar T_{eff} zero point since a perfectly solar T_{eff} is retrieved for the spectra of all the solar proxies (the Galilean satellites) (Table 7). The photometric and $H\alpha$ T_{eff} s scales therefore share the same zero point, and any systematic offset still to be gauged only remain in scale.

We note, however, that this good agreement should not be taken in an absolute sense. More sophisticated modeling of the solar Balmer profiles (Barklem et al. 2002) point to slight offsets between observations and theory, possibly due to both inconsistencies in the atmospheric models and the line broadening physics. Although very successful in recovering many observational features of the real Sun, even very recent 3D models (Pereira et al. 2013) still cannot reproduce the solar Balmer profiles perfectly. Our good internal consistency between photometric and $H\alpha$ T_{eff} scale should thus be regarded only in a relative sense for solar-type stars in the context of classical 1D modelling.

5.3. Uncertainties in the atmospheric parameters

Formal errors are estimated as follows: for the metallicity $[\text{Fe}/\text{H}]$, we adopt the average standard deviation of the distribution of abundances derived from the Fe I lines. This was $\sigma([\text{Fe}/\text{H}]) = 0.08$ dex, for the OPD spectra, and only $\sigma([\text{Fe}/\text{H}]) = 0.04$ dex, for the FEROS spectra (owing to the much better S/N of the latter). The error of the photometric T_{eff} is affected by the metallicity error. For two stars with S/N that are representative of the sample, we estimated the T_{eff} uncertainty due to the internal T_{eff} standard deviation of the color calibrations, adding the metallicity error. The values were $\sigma(T_{\text{eff}}) = 50$ K for the OPD spectra and $\sigma(T_{\text{eff}}) = 40$ K for the FEROS spectra. The error in $\log g$ was estimated, for the same three representative stars, by evaluating the variation in this parameter which produces a disagreement of 1σ between the abundances of Fe I and Fe II.

Table 5. Atmospheric parameters of the solar analogs with $V_{\text{Tycho}} \leq 8.0$. First col. is HD number; second and third cols. are the photometric and $H\alpha$ T_{eff} s (the former derived from the final adopted spectroscopic metallicity); fourth col. is the ionization surface gravity; and last col. is the spectroscopic metallicity.

HD	$T_{\text{eff}}^{\text{color}}$ (K)	$T_{\text{eff}}^{\text{H}\alpha}$ (K)	$\log g^{\text{ion}}$	$[\text{Fe}/\text{H}]$
Sun	5777	5777	4.44	+0.00
4308	5720	5695	4.44	-0.29
9986	5820	—	4.48	+0.09
13724	5820	5790	4.16	+0.24
19518	5780	—	4.34	-0.11
24293	5760	5690	4.10	-0.04
25874	5770	5770	4.40	+0.04
28821	5690	5680	4.58	-0.08
30495	5840	5800	4.36	+0.09
32963	5800	—	4.44	+0.08
35041	5810	—	4.46	-0.05
37773	5700	—	4.32	+0.04
66653	5840	—	4.40	+0.15
68168	5780	—	4.42	+0.11
71334	5770	5650	4.50	-0.06
73350	5830	5790	4.45	+0.14
88072	5800	—	4.24	+0.05
117939	5730	5800	4.44	-0.10
134664	5810	5830	4.36	+0.13
138573	5760	5740	4.42	+0.00
142072	5790	5790	4.46	+0.20
145825	5840	5830	4.52	+0.07
146233	5790	5800	4.48	-0.03
150248	5750	5750	4.38	-0.04
155114	5830	5810	4.46	-0.02
164595	5810	5770	4.67	-0.04
187237	5850	—	4.48	+0.16
189625	5870	5810	4.45	+0.27
190771	5840	5820	4.56	+0.19
207043	5790	5760	4.55	+0.07
214385	5730	—	4.24	-0.26

The result was $\sigma(\log g) = 0.20$ dex for the OPD and 0.15 for the FEROS data.

5.4. Masses and ages

For all stars with both a photometric and $H\alpha$ T_{eff} determination, we obtained a straight average to produce an internally more precise value of T_{eff} , where the errors of the determinations are very similar. A comparison of the two T_{eff} scales (Fig. 6) reveals excellent internal consistency: nearly all stars are contained within 1σ , and only one object, HD 71334, deviates by more than 2σ of the expected identity relation. The internal compounded error of the average T_{eff} for stars with both determinations is $\sigma \sim 30$ K and $\sigma \sim 35$ K, for FEROS and OPD stars, respectively. We adopt, conservatively, $\sigma(<T_{\text{eff}}>) = 40$ K in the following discussion. For the stars with both $H\alpha$ and photometric T_{eff} s, these averaged values were used to plot them in a grid of theoretical HR diagrams by the Geneva group (Schaller et al. 1992; Schaerer et al. 1993, and references therein). Only the photometric T_{eff} s were used for the other stars. Bolometric corrections were obtained from the tables of Flower (1996), and masses

Table 6. Same as Table 5 for the $8.0 < V_T \leq 9.0$ stars.

HD	$T_{\text{eff}}^{\text{color}}$ (K)	$T_{\text{eff}}^{\text{H}\alpha}$ (K)	$\log g^{\text{ion}}$	[FeH]
8291	5810	5860	4.30	+0.03
12264	5810	5810	4.54	+0.06
98649	5770	5780	4.63	-0.02
105901	5840	5850	4.50	-0.01
115382	5780	5790	4.40	-0.08
118598	5800	5730	4.52	+0.02
140690	5780	5790	4.40	+0.06
143337	5750	5760	4.36	-0.19
153458	5850	5810	4.44	+0.20
157750	5840	5850	4.54	+0.21
BD+15 3364	5800	5770	4.40	+0.07
191487	5820	5820	4.24	-0.01
202072	5750	5740	4.48	-0.17
211786	5780	5800	4.42	-0.09
216436	5750	5760	3.94	+0.04
221343	5800	5710	4.05	+0.04

Table 7. Same as Table 5 for the solar proxies and stars with UVB colors similar to the solar ones.

HD	$T_{\text{eff}}^{\text{color}}$ (K)	$T_{\text{eff}}^{\text{H}\alpha}$ (K)	$\log g^{\text{ion}}$	[FeH]
Ganymede	—	5780	—	—
Callisto	5770	5760	4.52	-0.04
Europa	5780	5770	4.48	-0.02
Sky	5770	—	4.56	-0.03
94340	5870	5840	3.99	+0.14
101563	5750	—	3.70	-0.12
105590	5790	5760	4.58	+0.02
111398	5780	—	4.28	+0.08
119550	5830	5780	3.98	+0.02
159222	5850	5830	4.34	+0.14
159656	5840	5850	4.32	+0.09
186408	5820	—	4.40	+0.11
221627	5790	5810	4.14	+0.17

and ages were interpolated in the diagrams. Astrometric surface gravities were derived from the well-known equation:

$$\log \left(\frac{g}{g_{\odot}} \right) = \log \left(\frac{M}{M_{\odot}} \right) + 4 \log \left(\frac{T_{\text{eff}}}{T_{\text{eff}_{\odot}}} \right) - \log \left(\frac{L}{L_{\odot}} \right). \quad (2)$$

In Tables 8, 9, and 10 we list astrometric surface gravities and their uncertainties (compounding errors in mass, T_{eff} , and luminosity in the equation above), along with bolometric magnitudes (and uncertainties), masses, and ages. It is seen that the internal errors of the astrometric surface gravities are much smaller than those of the ionization ones, and should be preferred in deciding the similarity of a given star to the Sun.

5.5. UV spectra

All stars observed in the UV at low resolution had their atmospheric parameters obtained from spectroscopic [Fe/H]s but HD 6512 and HD 28068. We performed a qualitative analysis of the UV stellar spectra divided by that of the solar proxy Ganymede. Our analysis was limited to verifying any significant structure in the ratio spectra differing from unity above the photon noise and normalization uncertainties (section 4.3), and we defer a more

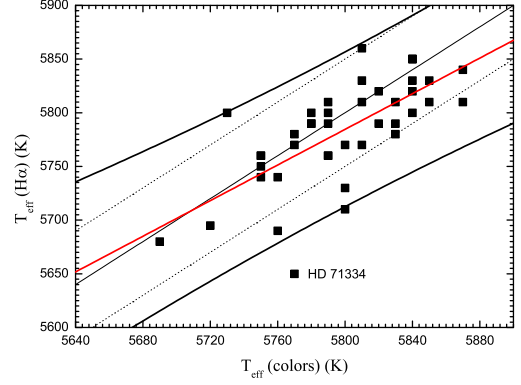


Fig. 6. Photometric and H α T_{eff} s compared. The thin black line is the identity relation, the red line is a linear least-squares fit, the two dotted lines bound the identity relation by 50 K, and the two thick black lines are the 95% confidence limits of the fit. The only star to deviate significantly from the identity is HD 71334.

complete quantitative investigation to a forthcoming paper. In Table 11 we list all results of this analysis, focused on the behavior of the CN and CH bandheads, respectively centered roughly at $\lambda 3870$ and $\lambda 4310$, and the Ca II H and K lines. It is apparent that nearly all analyzed stars have detectable or strong differences with respect to the solar spectrum. Particularly significant are the differences in the CH and CN bands, which are very sensitive to the stellar atmospheric parameters. Differences in the H and K line cores can be ascribed to different levels of chromospheric filling-in at the epoch of the observations and is not a direct flag of atmospheric parameters differing from the Sun's.

These data are particularly useful for selecting good UV analogs of the Sun. Such stars are desirable as solar proxies for observing comets, which generally have strong emission in the CH and CN transitions (e.g., Feldman et al. 2004; Grudzińska & Barbon 1968). In the case of cometary observations concentrated in the UV, the real issue is not whether the solar proxy has a strong color similarity to the Sun in the visible, but rather if its CH and CN features reproduce the solar ones well. Cometary emission usually has weak continua, and a good representation of the solar UV flux around the key molecular emission wavelengths is a necessity. Our list contains four stars that reproduce the solar CH and CN strengths very well, but not the solar fill-in in the H and K lines; and two additional stars that are indistinguishable from the Sun, within the errors, in the CN/CH and H and K wavelengths, a fact of some importance since the latter transitions lie in the wings of the λ CN and $\lambda 4056$ C₃ cometary emission lines for low-resolution observations. We discuss these objects in the next section, along with the solar analog and solar twin candidates.

6. Discussion

6.1. Different ways of masquerading as the Sun

Our spectroscopic analysis revealed a number of stars that not only possess a strong photometric similarity with the Sun pertaining the Paschen colors and the m_1 index, but not necessarily in the UV, as we discuss below. Many of these also have atmospheric parameters, T_{eff} , $\log g$, and [Fe/H] which are very similar to the solar ones within the errors. These objects can be con-

sidered as excellent solar analogs, are expected to have a spectral flux distribution very similar to the Sun's in the blue and red spectral range, and can be used for any observational procedure that requires removal of the solar spectrophotometric signature. The inferred masses cluster tightly around the solar value: indeed, in Tables 8 and 9, corresponding to our Hipparcos sample, only two stars have masses differing from solar by more than $0.1 M_{\odot}$, and 74% of the objects have masses within $\pm 0.05 M_{\odot}$ of the solar value. In Table 10, however, corresponding to stars selected solely by UBV similarity and presence in the lists of Hardorp (1982), various objects differ in mass from the Sun by more than this amount, illustrating the drawbacks of purely photometric criteria in identifying solar twins. On the other hand, the ages of all analyzed stars range very widely, from the zero-age main sequence (ZAMS) to values twice as old as the Sun. It is clear that stars with atmospheric parameters similar to the solar ones span a wide range of evolutionary states, a fact further stressing the differences between solar analogs and solar twins, and the importance of accurately determining atmospheric parameters and luminosities in order to successfully identify the latter.

Cross-checking the color similarity indices of Tables 1 and 2 with the spectroscopic parameters from Tables 5, 6 and 7, one gleams that a number of stars that are photometrically similar to the Sun appear so due to a combination of atmospheric parameters: they are either hotter/metal-rich or cooler/metal-poorer than the Sun. The most noteworthy of such objects among the brighter ($V_{\text{Tycho}} \leq 8.0$) sample stars are HD 9986, HD 66653, HD 73350, HD 117939, HD 134664, HD 187237, HD 189625, HD 190771. Examples among the fainter ($8.0 < V_{\text{Tycho}} \leq 9.0$) sample stars are HD 153458 and HD 157750. They can be successfully employed as photometric solar matches in a broad sense, for low-resolution spectroscopy of Solar System objects, but any analysis that can be influenced by subtle differences in the strength of metal lines should avoid these stars as solar proxies. They are well spaced in right ascension and span declinations from -64 to $+30$.

We divide our discussion of specific solar analogs and twins as follows. Purely photometric matches of the Sun, for which we could secure no spectroscopic data; solar analogs for which spectroscopic data are available, some of them qualifying as solar twin candidates; stars selected solely from UBV colors and presence in the Hardorp lists; and, lastly, stars matching the low resolution UV spectrum of the Sun. We close this section by presenting a new list of solar twin candidates having a high degree of photometric and spectroscopic resemblance to the Sun.

6.2. Purely photometric matches to the Sun

Stars for which no spectroscopic observations are available can be judged as good photometric analogs to the Sun solely by the S_C color similarity index and photometric atmospheric parameters, besides the Tycho absolute magnitude. In this way stars matching the solar colors can be revealed but not true solar analogs and twins. Considering only stars with $S_C \leq 1.50$, there are seven stars in the $V_{\text{Tycho}} \leq 8.0$ sample and 30 in the $V_{\text{Tycho}} > 8.0$ sample. In the brighter sample, one such object is the well-known solar twin HD 98618 (Meléndez et al. 2006), which is reliably recovered in our procedure. The other six stars are HD 28471, HD 70516, HD 88084, HD 139777, HD 158222, and HD 222143. Hardorp (1982) considered HD 70516 and HD 139777 as poor UV matches to the Sun. Further data may decide if they are good solar analog or twin candidates. All are good photometric matches to the Sun, and are also probable solar

analogs except for HD 139777, which is probably less luminous and cooler than the Sun, as well as poorer in metals. Particularly, HD 70516, HD 88084, HD 158222, and HD 222143 should be further investigated since their S_C plus the photometric T_{eff} and $[\text{Fe}/\text{H}]$ suggest a strong likeness to the Sun.

In the fainter sample, errors in the M_V^{Tycho} absolute magnitudes are greater and the objects correspondingly less interesting. Thirty stars are eligible as good solar photometric matches by having $S_C \leq 1.50$: HD 6512, HD 7678, HD 15632, HD 26736, HD 27857, HD 28068, HD 31130, HD 34599, HD 36152, HD 45346, HD 76332, HD 78660, HD 81700, HD 90322, HD 90333, HD 110668, HD 110869, HD 110979, HD 111938, HD 129920, HD 134702, HD 158415, HD 163441, HD 163859, HD 183579, HD 188298, HD 200633, HD 209262, HD 214635, and HD 215942. Most of the listed objects, additionally, have Tycho absolute magnitude in agreement with the solar one under a 2σ criterion, but for only three objects: HD 15632, HD 34599, and HD 36152. Two stars in this list have UV data, HD 6512 and HD 28068: they are very unlike the Sun in this wavelength range. This sample of 37 photometric matches to the Sun is widely scattered across the sky, has conveniently faint magnitudes, except perhaps for 10m-class telescopes, and may advantageously substitute Hardorp's lists in many useful contexts.

6.3. Solar analogs spectroscopically analyzed

Solar twins are automatically solar analogs, but not the other way round: bona fide stars successfully reproducing not only the solar spectrophotometric properties but also its atmospheric parameters and state of evolution must be gauged through spectroscopic analyses, to which we now turn. In the following discussion, it is important to keep in mind that: the $[\text{Fe}/\text{H}]$ uncertainty of the FEROS data is 0.04 dex, in contrast to 0.08 dex for the OPD data; that the 1σ internal uncertainty in T_{eff} is, approximately, 40K for stars with both photometric and $H\alpha$ determinations, but 50K if only one T_{eff} determination is available; and that the spectroscopic (ionization) $\log g$ (Tables 5, 6, and 7) is not a good discriminator between unevolved and evolved stars, but the astrometric $\log g$ (Tables 5, 6, and 7) is.

6.3.1. Brighter Hipparcos sample

The metric we adopt to judge a star as a good photometric match to the Sun is $S_C \leq 1.50$, a 3σ match. When available, we also consider activity data from the UV spectra (Table 11), as well as $H\alpha$ radiative losses from Lyra & Porto de Mello (2005): on their scale, the value of the solar flux is $F'_{H\alpha} = 3.44 \pm 0.45 (1\sigma)$, in $10^5 \text{ ergs}^{-1} \cdot \text{cm}^{-2} \cdot \text{sec}^{-1}$. We discuss first those stars with only one T_{eff} determination, for which conclusions carry less weight. In the brighter Hipparcos sample, there are four stars in this situation, all of them analyzed with FEROS data and all without a $H\alpha$ T_{eff} determination:

HD 9986 matches the Sun splendidly in its S_C index, but probably has higher metallicity than the Sun, $[\text{Fe}/\text{H}] = +0.09 \pm 0.04$ dex. Its absolute bolometric magnitude agrees with the solar one only very narrowly in a 2σ sense. It is a fair solar analog candidate, although not a clear solar twin candidate, yet it retains some possibility of a solar twin candidacy and should be further investigated.

HD 66653 is very probably metal-rich at $[\text{Fe}/\text{H}] = +0.15 \pm 0.04$ dex, but probably also hotter, which could explain its very good photometric similarity to the Sun. Its UV spectrum (see

section 6.5) supports just such a T_{eff} and $[\text{Fe}/\text{H}]$ match, balancing the spectroscopic and photometric properties to resemble the Sun's. Its chromospheric activity, judged by the H and K fill-in (Table 11) is equal to the solar one, and its absolute magnitude agrees with the solar one to nearly 1σ . It is thus a good photometric and UV match to the Sun, but not a real solar analog.

HD 88072 excellently matches the Sun in the photometric sense, but its absolute bolometric magnitude points to a more luminous and evolved star. Since its atmospheric parameters match the solar ones very closely, it appears to be a good solar analog candidate but not a solar twin case, but it is a close enough match to warrant further study.

HD 187237 is a very good solar photometric match, but it is very likely richer in metals than the Sun, at $[\text{Fe}/\text{H}] = +0.16 \pm 0.04$ dex. Its bolometric magnitude agrees well with the Sun's; yet its T_{eff} is probably hotter, explaining its position in the HR diagram very close to the ZAMS. A good photometric match, but neither a solar analog nor a solar twin candidate.

Concerning those stars in the brighter Hipparcos sample now with two T_{eff} determinations and therefore more reliable data, still adopting $S_C \leq 1.50$, as a metric and considering $H\alpha$ radiative losses from Lyra & Porto de Mello (2005), we have the following for each.

HD 24293 photometrically matches the Sun well, but it is possibly cooler than the Sun with its lower average $T_{\text{eff}} = 5735\text{K}$; its absolute bolometric magnitude is marginally solar at 2σ . Its UV data show the same chromospheric activity level as the Sun, a similar CN feature but a weaker CH feature, and its activity as judged by the $H\alpha$ line agrees with the solar level. We conclude it is a possible solar analog but an unlikely solar twin candidate.

HD 25874 has atmospheric parameters that are indistinguishable from solar besides a good S_C index, so it is an excellent solar analog. Its luminosity is higher than solar, reliably established with $\sigma(\text{Tycho } M_{\text{bol}}) = 0.03$ dex. Activity as judged by the $H\alpha$ line agrees with the solar level. Our conclusion is that it is not a solar twin candidate, but a prime solar analog.

HD 71334 is an excellent photometric match to the Sun and also has atmospheric parameters very close to solar. Its FEROS data and additional $H\alpha$ T_{eff} determination establish it as a good solar twin candidate since its luminosity matches the Sun's and it appears more inactive than the Sun in its H and K fill-in, while its activity level as judged by the $H\alpha$ line agrees with the Sun's. Its CH feature matches the Sun's, but the CN band is much weaker. This object warrants closer study.

HD 73350 photometrically matches the Sun very closely, but is probably richer in metals. It has both FEROS and OPD data, so this is probably a robust result. T_{eff} is solar but luminosity is lower with 2σ reliability. It lies close to the ZAMS and is a well known very active star (Lyra & Porto de Mello 2005) with much higher activity than the Sun, so it is a good photometric match but not a solar analog or twin candidate. We note that Hardorp (1982) did not consider it as a good UV match to the Sun.

HD 117939 is an excellent photometric match for the Sun and also has atmospheric parameters very close to solar. Since its luminosity also matches the Sun, it is a good solar twin candidate and deserves additional analysis, but its activity level from the $H\alpha$ line is higher than solar, $F'_{H\alpha} = 5.14 \pm 0.45$ (1σ).

HD 134664 is a close solar photometric match, but its metallicity $[\text{Fe}/\text{H}] = +0.13 \pm 0.08$ dex is not as good a match. T_{eff} is solar within the errors and the luminosity also matches the Sun's within 1σ , yet this star has the largest parallax error in the brighter Hipparcos sample. Its activity level from the $H\alpha$ line is

lower than solar, $F'_{H\alpha} = 2.33 \pm 0.45$ (1σ), and we conclude it is a probable solar analog but only a marginal solar twin candidate.

HD 138573 matches the Sun both photometrically and in its atmospheric parameters. Its luminosity also agrees with the solar one, and we conclude it is a good solar twin candidate, but for a much enhanced radiative loss in the $H\alpha$ line, $F'_{H\alpha} = 6.22 \pm 0.45$ (1σ), a value compatible with the Hyades cluster (Lyra & Porto de Mello 2005).

HD 146233 is the well known solar twin 18 Sco, HR 6060 and the only star in our Hipparcos sample brighter than $V^{\text{Tycho}} = 6.0$ (besides HD 30495). It is an excellent photometric match in the S_C index, its atmospheric parameters are solar within 1σ , and luminosity, mass, and age are all very close to solar. Our method establishes it firmly as a good solar twin candidate, lending confidence that additional candidates can be thus revealed. Nevertheless its UV features are not exactly solar: the CN band is weaker, and it appears slightly less active than the Sun in the H and K chromospheric fill-in. Its activity level from the $H\alpha$ line is slightly lower than solar, $F'_{H\alpha} = 2.71 \pm 0.45$ (1σ). We note that Hardorp (1982) did not consider HD 146233 as a close UV match to the Sun.

HD 150248 is an excellent photometric match to the Sun, and its atmospheric parameters and luminosity are sunlike within 1σ . Mass and age also agree very well, the $H\alpha$ radiative loss is solar within the errors, and thus it is still another very good solar twin candidate.

HD 164595 is also a good photometric match and has atmospheric parameters and luminosity within 1σ of the solar ones, the $H\alpha$ radiative loss is solar within the errors, and this star is another excellent solar twin candidate. Interestingly, Fesenko (1994) mentions this star as the one most resembling the Sun, photometrically, in his survey of 10 700 stars with WBVR magnitudes in the Moscow Photometric Catalog.

HD 189625 is a good photometric match but is probably metal-richer than the Sun, with $[\text{Fe}/\text{H}] = +0.27 \pm 0.08$ dex. It is also possibly hotter with $\langle T_{\text{eff}} \rangle = 5840\text{K}$, a likely explanation for its good photometric similarity. Absolute magnitude is marginally solar within 2σ , and mass is probably higher than solar. The $H\alpha$ radiative loss is slightly enhanced relative to solar, $F'_{H\alpha} = 4.55 \pm 0.45$ (1σ). It is neither a solar analog nor a solar twin case.

HD 190771 is probably hotter and more metal-rich than the Sun, but a good photometric match. Its UV data point to different CN and CH features and a much stronger chromospheric fill-in in the H and K lines, which agrees with its evolutionary position close to the ZAMS, despite absolute magnitude agreeing with the solar one. This is confirmed by a much higher chromospheric flux in the $H\alpha$ line, $F'_{H\alpha} = 9.09 \pm 0.45$ (1σ), a value compatible with the Hyades cluster or the very young Ursa Major moving group (Lyra & Porto de Mello 2005). Neither a solar analog nor a solar twin.

HD 207043 matches the Sun well photometrically and has atmospheric parameters within the Sun's at the 1σ level, and yet its absolute magnitude and evolutionary position point to a younger star that is much less evolved than the Sun, which is confirmed by its higher $H\alpha$ radiative loss, $F'_{H\alpha} = 4.76 \pm 0.45$ (1σ). Thus, a very good solar analog but no solar twin candidate.

The analysis of the atmospheric parameters, photometric similarities, and the evolutionary state of the brighter stars in the Hipparcos sample yields, therefore, three possible solar analogs, HD 9986 and HD 88072 (with only one T_{eff} determination) and HD 24293 (two T_{eff} determinations), as well as two definite very good solar analogs, HD 25874 (with higher luminosity than the Sun) and HD 207043 (with lower luminosity).

The real bounty, however, is three possible solar twin candidates, HD 71334, HD 117939, and HD 134664, and three new excellent solar twin candidates: HD 138573 (more active than the Sun, though), HD 150248, and HD 164595, besides a confirmation by our method of the known twin HD 146233, 18 Sco. Existing data for $H\alpha$ radiative losses, however, point to HD 117939 and HD 138573 having more enhanced chromospheric activity than the Sun.

6.3.2. Fainter Hipparcos sample

The stars of the fainter Hipparcos sample with $S_C \leq 1.50$ all have two T_{eff} determinations, and there are eight cases to discuss. Errors in absolute bolometric magnitude in this sample range from 0.10 to 0.15, and conclusions concerning solar twin candidacy carry correspondingly less weight than in the brighter Hipparcos sample.

HD 12264 is a good photometric match and has atmospheric parameters that all match the Sun's within 1σ . The absolute bolometric magnitude also matches the solar one, but its UV spectrum is very unlike the solar one, also presenting much stronger fill-in in the H and K lines, confirmed by a much higher chromospheric flux in the $h\alpha$ line, $F'_{H\alpha} = 6.12 \pm 0.45$ (1σ). Thus, it is a good solar analog but an unlikely solar twin candidate: the higher errors in luminosity could have masked an evolutionary state close to the solar one, but existing data on activity points towards a much younger star.

HD 98649 closely matches the Sun in photometry, atmospheric parameters, and absolute magnitude. It has no UV data, but the chromospheric flux gauged by $H\alpha$ is solar within 1σ . It is an excellent solar analog and a clear case for solar twin candidacy, besides one of the lowest errors in absolute magnitude in the fainter Hipparcos sample.

HD 115382 is a good photometric match and has atmospheric parameters very close to solar. Its $H\alpha$ chromospheric flux also matches the Sun's, and the absolute magnitude agrees with the solar value though only within a large error of 0.16. Thus it is a good solar analog and still a solar twin candidate.

HD 118598 is a nearly perfect photometric match to the Sun, besides having atmospheric parameters and absolute magnitude closely solar. Its $H\alpha$ radiative loss also agrees with the Sun's, and its absolute magnitude error of 0.12 dex is at the lower end in the fainter Hipparcos sample. We conclude it is a good solar analog and a solar twin candidate.

HD 140690 is an interesting case in that it was selected only in an incipient version of our Hipparcos color-absolute magnitude boxes. It is more luminous than the Sun, a good photometric match to it, and has atmospheric parameters that are indistinguishable from solar. It is clearly a very good solar analog but not a solar twin. In the UV, however, it is the closest match to the Sun in our sample, indistinguishable in the CN and CH features and also in the chromospheric fill-in in the H and K lines. Its $H\alpha$ radiative loss also matches the Sun's, and it is therefore a very good solar analog *and* a perfect UV analog. It is a very interesting spectrophotometric proxy of the Sun in a very wide wavelength range.

HD 153458 is an excellent photometric match to the Sun but is without doubt hotter and richer in metals, with $\langle T_{\text{eff}} \rangle = 5830\text{K}$ and $[\text{Fe}/\text{H}] = +0.20 \pm 0.08$ dex. Its absolute magnitude agrees very well with the Sun's, and the $H\alpha$ radiative loss is much higher than solar, $F'_{H\alpha} = 6.15 \pm 0.45$ (1σ). A good photometric match, but neither a solar analog nor a twin.

HD 157750 is a fair photometric match but is another case of a star hotter and richer in metals, with $\langle T_{\text{eff}} \rangle = 5845\text{K}$ and

$[\text{Fe}/\text{H}] = +0.21 \pm 0.04$ dex. Its absolute magnitude agrees very well with the Sun's, and the $H\alpha$ radiative loss is much higher than solar, $F'_{H\alpha} = 6.01 \pm 0.45$ (1σ). In the UV it has a solar CN feature but a weaker CH one, besides much stronger fill-in in the H and K lines, in good agreement with the $H\alpha$ data and an inferred evolutionary position close to the ZAMS. We deem it a reasonable photometric match, but neither a solar analog nor a twin.

Lastly, HD BD+15 3364 is a fair photometric match with atmospheric parameters, and absolute magnitude (with an error of 0.16) in very good agreement with the solar ones, and also a solar level of radiative losses in $H\alpha$. This object is clearly a good solar analog, and also a solar twin candidate: Hardorp (1982) mentioned it as a close match to the solar UV spectrum.

6.4. UVB similarity and Hardorp list stars

These stars were only selected on the basis of UVB similarity to the Sun and presence in Hardorp's lists, and are therefore not expected to have much resemblance to the solar atmospheric parameters and state of evolution. Five stars from Hardorp's lists were spectroscopically analyzed. HD 105590 has atmospheric parameters close to solar (but only one T_{eff} determination) but a very unsolar-like S_C index: Hardorp (1982) regarded it, though, as a solar analog. HD 186408 was not considered by Hardorp as a close case as solar analogs go, but it is photometrically very similar to the Sun in the S_C index: its T_{eff} is close to solar (but this is judged from a single determination) and its $[\text{Fe}/\text{H}]$ appears higher than solar within the uncertainty. Previous analyses (Friel et al. 1993; Porto de Mello & da Silva 1997) confirm this star as a good analog but not a solar twin. Two other Hardorp stars with S_C indices close to solar turn out not to be solar analogs at all: on the one hand, HD 159222, considered a close solar UV match by Hardorp, is hotter, richer in metals, and more evolved than the Sun; on the other hand, HD 101563, considered by Hardorp as a bad UV match to the Sun, is much more massive, more evolved, and poorer in metals. One more Hardorp star, but only judged by its UV spectroscopy, is HD 28255: it does not resemble the Sun in either its CN and CH features or its S_C index.

Eight stars were selected by having solar UVB colors within the adopted errors. Four of these have only UV spectroscopy, and only one, HD 16141 turns out to have CN and CH features resembling the Sun's (but a weaker chromospheric fill in the Ca II H and K lines; we also note that Hardorp (1982) found it as a bad UV match to the Sun, at variance with us. Its S_C index is, however, very non-solar. The remaining four stars with solar UVB colors were spectroscopically analyzed, but none are photometrically similar to the Sun or has a strong resemblance in atmospheric and/or evolutionary parameters.

The results for these stars further illustrate the danger of choosing solar analogs from scarce data.

6.5. Ultraviolet matches to the solar spectrum

There are 37 stars that could be compared to the Sun in the UV range at low resolution (Table 11). Still undiscussed are HD 26767 and HD 43180 from the fainter Hipparcos sample, and for which no additional data is available but for the UV spectroscopy: none of them closely resemble the Sun in their UV features or have a sunlike S_C index. We found four stars with both a strong S_C similarity to the Sun and solar-like CN/CH features. Two of these have already been discussed above: HD 66653 is

photometrically similar to the Sun, but this is probably owing, as seen above, to a combination of higher T_{eff} and $[\text{Fe}/\text{H}]$. Its UV features are very similar to the Sun, including the chromospheric fill-in in the HK lines, and it is proposed as a good solar proxy in the UV. The other one, HD 140690, is a very good solar analog strongly resembling the Sun in its S_C index, besides having the UV spectrum indistinguishable from the solar one. It is a rare case in which the atmospheric parameters, the Paschen colors, and the UV spectral features are very solar-like, and it can therefore be proposed as an excellent photometric analog of the Sun in a wide wavelength range, a very interesting object indeed. Nevertheless it is not a solar twin candidate, since it is more luminous and probably more evolved than the Sun.

There are two other stars with $S_C \leq 1.50$ and very solar-like UV features. The first is HD 159656. It was selected from Hardorp's lists, is a good photometric match to the Sun, but is definitely hotter than the Sun, as well as probably being richer in metals. Hardorp (1982) did not mention it as a good solar match in the UV. Its chromospheric H and K fill-in is also much stronger than the Sun's. Secondly we have HD 221343: it is not a good photometric match, its atmospheric parameters are determined from poor S/N data, and its H and K emission is much stronger than solar. Our results suggest it is probably hotter and richer in metals than the Sun. Our analysis thus presents only HD 140690 as a truly good photometric analog to the Sun also with a UV spectrum that is strongly solar-like.

Two other objects merit comment: HD 16141, already discussed above, is a very poor photometric match to the Sun, and it only has UV spectroscopic data, but its CN and CH features are indistinguishable from solar. Its H and K emission is weaker than solar. Its purely photometric T_{eff} and $[\text{Fe}/\text{H}]$ point to its being cooler and metal-poorer than the Sun. Finally, HD 68168 is not a good photometric solar match, but again it has very sun-like CN and CH features, yet weaker H and K fill in. Our spectroscopic analysis suggests it is richer in metals than the Sun but it possesses solar T_{eff} within errors, based on only one T_{eff} determination.

The UV wavelength range is thus a very fine discriminator of solar analogs and it is apparent that the CN and CH features, even in low resolution, can bring out differences in T_{eff} and $[\text{Fe}/\text{H}]$ between stars and the Sun which are, at best, very hard to reveal by spectroscopic analyses. The UV approach clearly warrants deeper analysis with more data, which we plan to present in a forthcoming paper.

Good solar twins appear unequivocally linked to a fair photometric similarity to the Sun as inferred from our S_C index. In Figure 7 we plot our T_{eff} s versus the spectroscopic $[\text{Fe}/\text{H}]$ s, shown as S_C contours, for two different regimes of color similarity to the Sun: all analyzed stars and only those with $S_C \leq 3.0$. This plot illustrates in greater detail what has already been gleaned from Figure 3: stars with atmospheric parameters very similar to the Sun's automatically produce high similarity in S_C as well, but there is a locus in which stars with T_{eff} and $[\text{Fe}/\text{H}]$ values quite different from solar may mimic a high degree of similarity to the Sun. Roughly, for every +0.1 dex increase in $[\text{Fe}/\text{H}]$, a parallel +36 K increase in T_{eff} leaves S_C unchanged. A spectroscopic analysis is then needed to remove the degeneracy and separate true solar analogs from stars merely mimicking a strong spectrophotometric similarity to the Sun.

6.6. New solar twin candidates

In Table 12 we list ten stars pointed out by our survey as interesting new solar twin candidates, along with the Sun and the known

twin HD 146233 (a.k.a. 18 Sco) for comparison. At the top of the list there are six stars from the brighter Hipparcos sample, three of them "probable" twins, and three only "possible" twins, with weaker claims. The atmospheric and evolutionary parameters are shown with their errors (excepting mass, for which errors are usually 0.02-0.03 solar masses, and age, for which errors are generally so large as to preclude definite conclusions), and we also provide comments on the chromospheric activity level. The last four entries in the table correspond to stars from the fainter Hipparcos sample, two of these being "probable" solar twins, and two more classified as "possible" twins. The very best candidates are HD 150248 and HD 164595, which match the Sun well in every parameter plus the level of chromospheric activity and which belong to the brighter Hipparcos sample, so have reduced errors in parallax and luminosity. In the fainter Hipparcos sample, HD 98649 and HD 118598, which also match the Sun perfectly, have reasonable uncertainties in luminosity, and are also chromospherically inactive. These stars will be subjected to a more detailed scrutiny, including the lithium abundance and additional chromospheric activity indicators, in a forthcoming paper.

HD 146233, 18 Sco, remains the only one bright ($V^{\text{Tycho}} \leq 6.0$) solar twin candidate or confirmed solar twin known so far. We may ask, given the completeness of the data used as input in our survey, what the probability is of finding still other solar twin candidates among the $V^{\text{Tycho}} \leq 8.0$ stars. This can be roughly estimated as follows. Among the G-type, $V^{\text{Tycho}} \leq 8.0$ stars in the Hipparcos catalog, completeness in the $(B - V)^{\text{Tycho}}$ color is 95%. We selected 52 stars for our survey within this magnitude limit, and supposing that 5% are missing, there are 2.6 stars we failed to select. We spectroscopically analyzed 30 stars among the 52 star sample, and found four "probable" solar twin candidates, which, plus the previously known solar twins HD 146233 and HD 98618, gives a total of six solid twin candidates. Thus, among 30 analyzed stars, we have six twin candidates, a rate of 20%. There are, as a consequence, $2.6/5 \sim 0.5$ stars missing from our survey, owing to incompleteness, which are probable twin candidates. Now, because there are seven stars in our brighter sample for which we could not secure spectroscopic data (leaving aside HD 98618, accepted as a known twin) and which have $S_C \leq 1.50$, there remains a possibility that ~ 1.4 of these are probable twins that we have so far failed to identify. Given that among 52 stars selected for the brighter Hipparcos sample, only two, or 3.8%, are brighter than $V^{\text{Tycho}} = 6.0$, there is at best $(1.4+0.5)$ times $0.038 \sim 0.076$ stars with $V^{\text{Tycho}} \leq 6.0$, which are probable solar twin candidates, and we failed either to select in the first place or to analyze spectroscopically. This figure is probably overestimated since completeness in the Hipparcos catalog falls off between $V^{\text{Tycho}} \leq 6.0$ stars and our magnitude limit $V^{\text{Tycho}} = 8.5$, meaning that it is very unlikely that solar twins any brighter than HD 146233 remain undetected.

7. Conclusions

We have reported a photometric and spectroscopic survey of solar twin stars that is photometrically all-sky, complete out to 40 pc, and partially complete out to 50 pc, and involving 136 solar-type stars. We derived photometric T_{eff} s and photometric metallicities $[\text{Fe}/\text{H}]$ for the whole sample and ranked these stars relative to the Sun by means of a photometric similarity index. Spectroscopic parameters based on moderate-resolution, high-S/N spectra were also derived for a subsample of 55 stars, and for these we derived spectroscopic metallicities, photometric T_{eff} s based on the spectroscopic metallicities, and

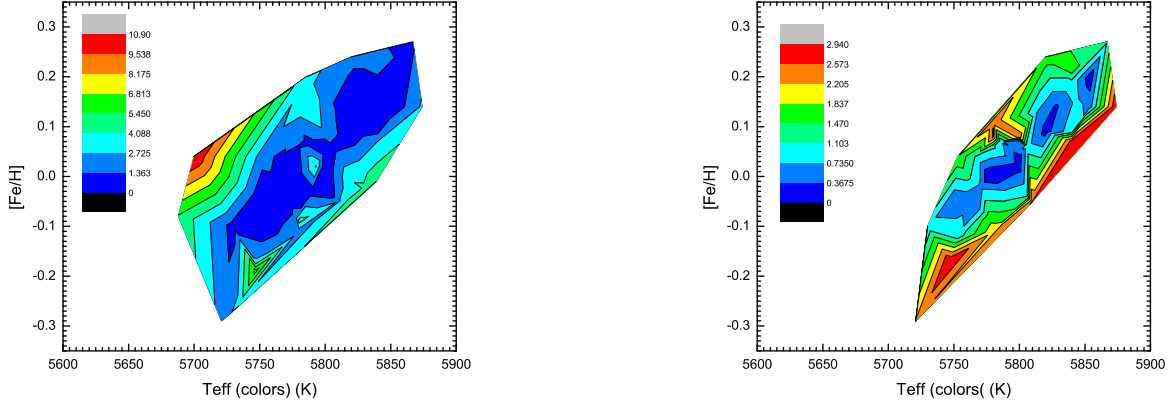


Fig. 7. *Left.* The color similarity index S_C plotted *versus* the final photometric T_{eff} s (obtained from the spectroscopic $[\text{Fe}/\text{H}]$ s) and the spectroscopic $[\text{Fe}/\text{H}]$ s for all spectroscopically analyzed stars. The vertical colored bar is coded by the S_C values; note that the scale of the coding is different between the two plots. *Right.* The same as the left panel, but for the stars with $S_C \leq 3.0$. It is clear that a combination of hot/metal rich and cool/metal poor parameters defines an area of good photometric similarity to the Sun, and also that the stars with the highest color similarity to the Sun have atmospheric parameters more tightly clustered around the solar values.

Table 12. New solar twin candidates identified in this work. Columns 2, 3, and 4 give the final atmospheric parameters T_{eff} (K), $[\text{Fe}/\text{H}]$ and $\log g$, respectively. Column 5 presents the apparent magnitude in the Tycho band, and column 6 the color similarity index S_C . Columns 7, 8, and 9 provide the absolute bolometric magnitude in the Tycho band, mass, and age respectively. The tenth column comments on the chromospheric activity level as compared to the Sun, when available, and gives relevant remarks.

HD	$T_{\text{eff}} \pm \sigma$ [K]	$\log g^{\text{astr}} \pm \sigma$	$[\text{Fe}/\text{H}] \pm \sigma$	V^{Tycho}	S_C	$M_{\text{bol}}^{\text{Tycho}} \pm \sigma$	Mass [M_{\odot}]	Age [Gyr]	remarks
Sun	5777	4.44	+0.00	–	0.00	4.81 ± 0.03	1.00	4.6	–
71334	5710 ± 30	4.44 ± 0.07	-0.06 ± 0.04	7.9	0.22	4.84 ± 0.08	0.97	5.1	inactive; possible twin
117939	5765 ± 40	4.42 ± 0.06	-0.10 ± 0.08	7.4	0.83	4.87 ± 0.06	0.94	6.1	active; possible twin
134664	5820 ± 40	4.46 ± 0.08	$+0.13 \pm 0.08$	7.8	0.76	4.78 ± 0.11	1.04	2.6	inactive; possible twin
138573	5750 ± 40	4.41 ± 0.06	$+0.00 \pm 0.08$	7.3	1.24	4.77 ± 0.06	0.98	5.6	very active; probable twin
146233	5795 ± 30	4.42 ± 0.05	-0.03 ± 0.04	5.6	0.78	4.77 ± 0.03	0.98	5.0	known solar twin
150248	5750 ± 40	4.39 ± 0.06	-0.04 ± 0.08	7.1	0.52	4.75 ± 0.07	0.96	6.2	inactive; very probable twin
164595	5790 ± 40	4.44 ± 0.05	-0.04 ± 0.08	7.1	1.11	4.79 ± 0.05	0.99	4.5	inactive; very probable twin
98649	5775 ± 30	4.44 ± 0.08	-0.02 ± 0.04	8.1	0.58	4.84 ± 0.10	0.98	4.7	inactive; probable twin
115382	5775 ± 30	4.39 ± 0.10	-0.08 ± 0.04	8.5	1.16	4.73 ± 0.16	0.96	6.1	inactive; possible twin
118598	5755 ± 40	4.44 ± 0.08	$+0.02 \pm 0.08$	8.3	0.12	4.78 ± 0.12	1.01	4.3	inactive; probable twin
BD+15 3364	5785 ± 30	4.44 ± 0.10	$+0.07 \pm 0.08$	8.2	1.38	4.77 ± 0.16	1.02	3.8	inactive; possible twin

T_{eff} s derived from the fitting of $H\alpha$ profiles. Masses and ages were also provided for the spectroscopically analyzed stars. Low-resolution UV spectra are available for a subsample of 37 stars, allowing the evaluation of their relative similarity with respect to the Sun in the CH and CN molecular features, as well as the chromospheric fill-in in the Ca II H and K lines. Our conclusions are as follows.

1) The color-similarity index is very successful in selecting stars having colors *and* atmospheric parameters that are very similar to the solar ones. A large number of new solar

analogs were identified, and these objects proposed as useful spectrophotometric proxies of the Sun, satisfying various degrees of accuracy and covering essentially all of the sky with a magnitude limit $V^{\text{Tycho}} \leq 8.5$. They should be particularly useful as solar proxies for photometry and/or low-resolution spectroscopy of Solar System bodies.

2) Two stars were also shown to have all the near UV spectral features indistinguishable from solar and were suggested as solar UV templates. Only one, however, HD 140690, possesses atmospheric parameters equal to the Sun's, making it a solar

Table 8. Parameters derived from the HR diagram analysis for the $V^{\text{Tycho}} \leq 8.0$ stars. First column shows the HD number, second column the astrometric surface gravity and uncertainty, third column the absolute bolometric magnitude in the V^{Tycho} band and uncertainty, and fourth and fifth columns are the mass (in solar units) and age (in Gyr), respectively. The Sun is shown in the first row for comparison.

HD	$\log g^{\text{astr}}$	M_{bol}	Mass (M_{\odot})	Age (Gyr)
Sun	4.44	4.81 ± 0.03	1.00	4.6
4308	4.37 ± 0.05	4.82 ± 0.03	0.88	9.2
9986	4.43 ± 0.05	4.73 ± 0.05	1.02	3.4
13724	4.44 ± 0.07	4.72 ± 0.09	1.06	2.2
19518	4.40 ± 0.07	4.76 ± 0.10	0.96	6.1
24293	4.39 ± 0.07	4.70 ± 0.09	0.97	6.3
25874	4.39 ± 0.05	4.69 ± 0.03	0.99	1.5
28821	4.35 ± 0.07	4.73 ± 0.09	0.93	8.0
30495	4.50 ± 0.05	4.83 ± 0.04	1.05	2.6
32963	4.48 ± 0.07	4.85 ± 0.09	1.03	2.5
35041	4.45 ± 0.07	4.83 ± 0.09	0.99	4.0
37773	4.39 ± 0.08	4.78 ± 0.10	0.97	6.7
66653	4.46 ± 0.06	4.75 ± 0.06	1.05	2.2
68168	4.41 ± 0.07	4.72 ± 0.09	1.02	4.4
71334	4.44 ± 0.07	4.84 ± 0.08	0.97	5.1
73350	4.51 ± 0.06	4.90 ± 0.06	1.05	ZAMS
88072	4.40 ± 0.07	4.67 ± 0.09	1.01	5.0
117939	4.42 ± 0.06	4.87 ± 0.06	0.94	6.1
134664	4.46 ± 0.08	4.78 ± 0.11	1.04	2.6
138573	4.41 ± 0.06	4.77 ± 0.06	0.98	5.6
142072	4.44 ± 0.07	4.77 ± 0.10	1.03	2.8
145825	4.51 ± 0.06	4.89 ± 0.05	1.05	ZAMS
146233	4.42 ± 0.05	4.77 ± 0.03	0.98	5.0
150248	4.39 ± 0.06	4.75 ± 0.07	0.96	6.2
155114	4.46 ± 0.07	4.81 ± 0.08	1.00	2.7
164595	4.44 ± 0.05	4.79 ± 0.05	0.99	4.5
187237	4.50 ± 0.05	4.85 ± 0.04	1.06	ZAMS
189625	4.47 ± 0.07	4.72 ± 0.08	1.09	1.0
190771	4.50 ± 0.05	4.85 ± 0.03	1.06	ZAMS
207043	4.52 ± 0.06	4.95 ± 0.07	1.04	ZAMS
214385	4.40 ± 0.07	4.88 ± 0.10	0.87	7.8

analog, and it also photometrically matches the Sun well in the Paschen continuum colors and the Strömgren m_1 index. It was therefore proposed as a prime solar analog from the UV out to the visible wavelength range. Other stars were shown to resemble the Sun in the UV owing to a fortuitous composition of atmospheric parameters, and care should be exercised in selecting stars to represent the Sun *both* in the UV and visible ranges. Good UV solar proxies may be particularly important for the observation of UV emission lines in comets.

3) The spectroscopic and evolutionary analysis revealed five new “probable” solar-twin candidates, plus five new “possible” twin candidates, besides successfully identifying two previously known solar twins, HD 146233 and HD 98618. The four probable new solar twin candidates, HD 98649, HD 118598, HD 150248, and HD 164595, have atmospheric and evolutionary parameters indistinguishable from the solar ones within the uncertainties, besides a low level of chromospheric activity, so they clearly warrant closer scrutiny.

In a forthcoming paper, we will discuss these objects in more detail, including a multi-element abundance analysis, additional criteria to determine T_{eff} , a deeper study of their

Table 9. Same as Table 8 for the $8.0 < V^{\text{Tycho}} \leq 9.0$ stars.

HD	$\log g^{\text{astr}}$	M_{bol}	Mass (M_{\odot})	Age (Gyr)
8291	4.45 ± 0.10	4.78 ± 0.16	1.02	3.9
12264	4.45 ± 0.08	4.80 ± 0.12	1.02	3.4
98649	4.44 ± 0.08	4.84 ± 0.10	0.98	4.7
105901	4.43 ± 0.08	4.74 ± 0.12	0.99	3.8
115382	4.39 ± 0.10	4.73 ± 0.16	0.96	6.1
118598	4.44 ± 0.08	4.78 ± 0.12	1.01	4.3
140690	4.39 ± 0.08	4.66 ± 0.11	1.01	5.3
143337	4.35 ± 0.09	4.72 ± 0.14	0.91	7.9
153458	4.50 ± 0.08	4.82 ± 0.11	1.07	ZAMS
157750	4.50 ± 0.09	4.84 ± 0.15	1.06	ZAMS
191487	4.43 ± 0.10	4.74 ± 0.15	1.00	4.5
202072	4.35 ± 0.08	4.70 ± 0.12	0.92	7.9
211786	4.46 ± 0.08	4.89 ± 0.10	0.97	4.3
216436	4.37 ± 0.09	4.65 ± 0.11	0.99	6.1
221343	4.44 ± 0.09	4.78 ± 0.13	1.01	4.0
BD+15 3364	4.44 ± 0.10	4.77 ± 0.16	1.02	3.8

Table 10. Same as Table 8 for the stars with UBV colors similar to the solar ones. HD 105590 has a very large parallax error, and no age was derived for it.

HD	$\log g^{\text{astr}}$	M_{bol}	Mass (M_{\odot})	Age (Gyr)
94340	4.19 ± 0.08	3.98 ± 0.10	1.14	4.9
101563	3.89 ± 0.10	3.24 ± 0.08	1.22	3.6
105590	4.34 ± 0.28	4.54 ± 0.60	1.00	–
111398	4.46 ± 0.08	4.84 ± 0.12	1.02	3.3
119550	3.85 ± 0.09	3.01 ± 0.13	1.31	2.9
159222	4.43 ± 0.05	4.66 ± 0.04	1.05	2.8
159656	4.36 ± 0.07	4.54 ± 0.09	1.03	4.4
186408	4.25 ± 0.05	4.29 ± 0.04	1.02	2.4
221627	3.95 ± 0.08	3.36 ± 0.10	1.23	3.6

spectroscopic chromospheric indicators, the determination of their kinematics, and a more detailed evolutionary analysis.

APPENDIX A: A Metallicity-dependent IRFM T_{eff} calibration for solar-type stars

Theoretical calculations in stellar modeling predict relations between structural quantities that see little change during stellar evolution, such as mass and metallicity, and others that vary extensively, such as effective temperature, radius, and luminosity. These quantities are not straightforward to determine, and their match to accessible observational data such as colors lies at the heart of stellar astrophysics. The effective temperature is the most basic stellar parameter that affects the model atmosphere abundance analysis of stars. Moreover, at least for nearby stars for which very precise parallaxes are presently available (ESA 1997), the T_{eff} is now the single most important source of error in placing stars in theoretical HR diagrams.

The aim of the T_{eff} calibrations presented here is not to emulate or be an alternative to the many excellent resources available nowadays (e.g., Casagrande et al. 2010, 2006; Masana et al. 2006; Ramírez & Meléndez 2005b), but to provide, in the context of a solar analog search, a solid base for comparing photometric T_{eff} s to those inferred from spectroscopy and Balmer line profiles with the specific aim of better distinguishing small T_{eff} differences between the Sun and candidate solar analogs and

Table 11. Qualitative assessment of the stellar spectral feature deviations from the solar spectrum, expressed as measured in the ratio spectra between the stars and Ganymede. In the second and third columns we classify the strength of ratio features around the $\lambda 3870$ CN bandheads and the $\lambda 4310$ CH bandhead, respectively. In the fourth column, the chromospheric filling in the Ca II H and K lines is given.

HD	CN	CH	H & K
4308	much weaker	solar	weaker
6512	stronger	weaker	solar
8291	weaker	weaker	stronger
9562	much weaker	much weaker	much weaker
12264	weaker	weaker	much stronger
13724	stronger	solar	much stronger
16141	solar	solar	weaker
19467	much weaker	solar	much weaker
19518	much weaker	weaker	solar
24293	solar	weaker	solar
26767	much weaker	much weaker	much stronger
28068	much weaker	much weaker	much stronger
28255	much weaker	weaker	solar
28821	much weaker	solar	solar
32963	solar	weaker	solar
35041	much weaker	much weaker	much stronger
37773	much stronger	weaker	solar
43180	much weaker	much weaker	stronger
66653	solar	solar	solar
68618	solar	solar	much weaker
71334	much weaker	solar	weaker
140690	solar	solar	solar
143337	much weaker	solar	solar
146233	weaker	solar	weaker
155114	much weaker	much weaker	much stronger
157750	solar	weaker	much stronger
159222	much weaker	solar	stronger
159656	solar	solar	much stronger
189625	solar	stronger	weaker
190771	much weaker	weaker	much stronger
191487	much weaker	much weaker	much stronger
202072	much weaker	solar	solar
211786	much weaker	weaker	solar
214385	much weaker	weaker	weaker
216436	weaker	solar	weaker
221343	solar	solar	much stronger
221627	much weaker	weaker	much weaker

twins. To apply differential philosophy to the greatest possible extent and to ensure maximum homogeneity, it is desirable that all T_{eff} scales employed in the present study be tied to a similar suite of model atmospheres, in our case the MARCS system of model atmospheres, as described by Edvardsson et al. (1993, see <http://marcs.astro.uu.se>; Gustafsson et al. 2008).

An “ideal” direct T_{eff} calibration should be based on an extensive set of precise measurements of bolometric fluxes and angular diameters and be independent of any grid of model atmospheres. Among the various “indirect” methods employed so far alternatively, one of the most advantageous is the infrared flux method (IRFM) (originally described by Blackwell & Shallis 1977; Blackwell et al. 1986) since it relies only weakly on theoretical representations of stellar atmospheres. Details on the method are given by Blackwell et al. (1986, 1990).

Some recent determinations of the relation between T_{eff} (IRFM) and stellar colors (e.g., Masana et al. 2006; Casagrande et al. 2010; Ramírez & Meléndez 2005b) report

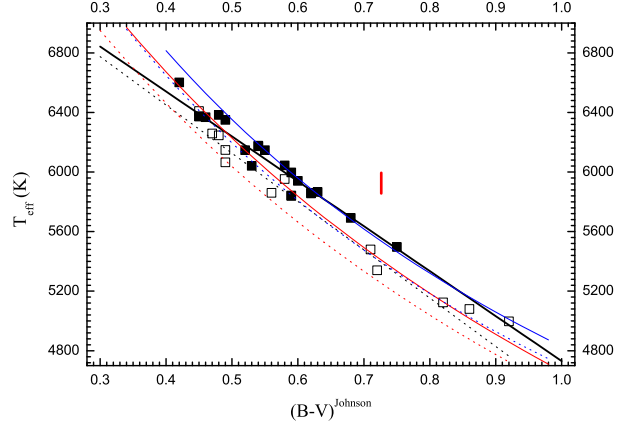


Fig. 1. Figure A.1. Our calibration for the $(B - V)_{\text{Johnson}}$ index compared to literature results. The adopted 1σ T_{eff} error (see text) is shown as the thick red vertical bar. Full squares are stars with $[\text{Fe}/\text{H}] > +0.10$ dex, open squares with $[\text{Fe}/\text{H}] < +0.10$ dex. The black full and dotted lines refer, respectively, to our calibrations for $[\text{Fe}/\text{H}] = +0.00$ and $[\text{Fe}/\text{H}] = -0.50$; the red and blue lines follow the same $[\text{Fe}/\text{H}]$ convention for the relations of Alonso et al. (1996) and Casagrande et al. (2006), respectively.

that the T_{eff} scale of FGK stars is established to better than $\sim 1\%$ or ~ 60 K. Casagrande et al. (2006) find good agreement between empirical and synthetic colors both for the ATLAS and MARCS families of models in the visible, but less so in the infrared, and also report, concurrently with Masana et al. (2006) and da Silva et al. (2012), that good agreement is realized between the spectroscopic and photometric T_{eff} scales for solar-type stars, although disagreements of a few percent are found between different authors. However, much equally recent work (e.g., Ramírez et al. 2007; Ramírez & Meléndez 2005a; Yong et al. 2004) state that the spectroscopic T_{eff} scale of solar-type stars is hotter than the photometric one by ~ 100 K. This is in line with Porto de Mello et al. (2008), who find, in a detailed analysis of the very well-studied double system α Cen AB, a discrepancy between the spectroscopic T_{eff} scale and those from photometry and the fitting of Balmer line profiles. Nonetheless Ramírez & Meléndez (2005a) and da Silva et al. (2012) obtain good consistency between photometric T_{eff} s and those derived from the fitting of Balmer line profiles. Despite recent efforts (Casagrande et al. 2010) to clarify these offsets, a somewhat confusing picture still emerges from the literature concerning the overall agreement of the photometric, Balmer line, and spectroscopic T_{eff} scales over a wide parameter range; fortunately, much better consistency can be found near the solar parameters (da Silva et al. 2012), thus the broader issues of the T_{eff} scale of FGK stars need not concern us here.

Selection of photometry, IRFM T_{eff} and $[\text{Fe}/\text{H}]$ data

Our choice of older IRFM T_{eff} determinations is based mainly on the goal of realizing strict consistency with the MARCS models used in our $[\text{Fe}/\text{H}]$ (section 5.1) and Balmer line T_{eff} (section 5.2) determinations, and therefore our emphasis was not on the latest resources. The adopted T_{eff} values, given in Table A.1, come from Saxner & Hammarbäck (1985) and Blackwell et al. (1991), who used MARCS models in their

Table 1. Table A.1. Objects selected for the T_{eff} versus color calibrations. Sources for $(b - y)$ and β are given in Table 14. The $(R - I)$, $(V - R)$, $(V - I)$, and $(V - K)$ colors are all in the Johnson system (Glass 1974; Johnson 1964; Johnson et al. 1966, 1968). When only narrow-band $(V - K_n)$ from Selby et al. (1988) is available, they have been transformed to Johnson $(V - K)$ using the relations provided by these same authors. The MK spectral type and Johnson $(B - V)^J$ colors were taken from the Bright Star Catalogue (Hoffleit & Jaschek 1991). The Tycho $(B - V)^T$ colors come from ESA (1997). The third column gives T_{eff} as obtained by Blackwell et al. (1991) (1) or Saxner & Hammarbäck (1985) (2). When both authors provide a T_{eff} value, the straight average is tabulated.

HR	HD	Spectral type	T_{eff} (IRFM) (K)	[Fe/H]	$(B - V)^J$	$(B - V)^T$	$(R - I)$	$(V - R)$	$(V - I)$	$(V - K)$	$(b - y)$	β
33	693	F7V	6148 (2)	-0.55	0.487	0.519	—	—	—	1.23	0.326	2.617
98	2151	G2IV	5860 (2)	-0.17	0.618	—	0.34	0.50	0.84	1.48	0.394	2.597
244	5015	F8V	6042 (2)	-0.08	0.540	0.610	0.30	0.48	0.78	1.28	0.346	2.613
417	8799	F5IV	6547 (1)	—	0.421	0.463	0.23	0.41	0.64	1.07	0.288	2.672
458	9826	F8V	6177 (1/2)	+0.12	0.536	0.589	0.29	0.46	0.75	1.25	0.344	2.629
483	10307	G1.5V	5856 (2)	-0.02	0.618	0.686	0.33	0.53	0.86	1.39	0.389	2.604
509	10700	G8V	5341 (1)	-0.50	0.727	—	0.42	0.62	1.09	1.82	0.449	2.555
544	11443	F6IV	6350 (1)	+0.06	0.488	0.526	0.28	0.42	0.70	1.18	0.316	2.637
740	15798	F4IV	6409 (2)	-0.19	0.454	0.478	0.27	0.41	0.68	1.12	0.297	2.640
799	16895	F8V	6373 (2)	+0.02	0.514	0.541	0.30	0.46	0.76	1.15	0.326	2.625
818	17206	F5/F6V	6350 (2)	+0.05	0.481	0.515	0.27	0.43	0.70	1.14	0.328	2.646
937	19373	G0V	5997 (1/2)	+0.08	0.595	0.668	0.29	0.53	0.82	1.36	0.201	2.605
996	20630	G5Vv	5692 (1)	+0.06	0.681	0.756	0.36	0.57	0.93	1.52	0.420	2.585
1101	22484	F9V	5953 (1/2)	-0.13	0.575	0.626	0.32	0.49	0.81	1.36	0.370	2.608
1325	26965	K1V	5125 (1)	-0.32	0.820	—	0.45	0.69	1.14	2.02	0.487	2.543
1543	30652	F6V	6373 (2)	+0.09	0.484	0.504	0.26	0.42	0.68	1.12	0.299	2.651
1729	34411	G2IV-V	5866 (1/2)	+0.11	0.630	0.696	0.32	0.53	0.85	1.43	0.389	2.598
1983	38393	F6V	6259 (2)	-0.12	0.481	0.530	0.26	0.45	0.71	1.16	0.315	2.634
2047	39587	G0V	5839 (2)	-0.08	0.594	0.659	0.31	0.51	0.82	1.44	0.378	2.601
2943	61421	F5IV-V	6601 (2)	-0.07	0.432	—	0.23	0.42	0.65	1.02	0.272	2.671
4054	89449	F6IV	6374 (2)	-0.15	0.452	0.503	0.23	0.45	0.68	1.15	0.301	2.654
4540	102870	F9V	6147 (2)	+0.11	0.518	0.613	0.28	0.48	0.76	1.27	0.354	2.629
4785	109358	G0V	5842 (2)	-0.20	0.588	0.655	0.31	0.54	0.85	1.43	0.385	—
5072	117176	G2.5Va	5480 (1)	-0.11	0.714	0.804	0.39	0.61	1.00	1.74	0.454	2.576
5185	120136	F6IV	6383 (2)	-0.04	0.508	0.534	0.24	0.41	0.65	1.11	0.313	2.656
5235	121370	G0IV	6044 (1)	+0.21	0.580	0.670	0.29	0.44	0.73	1.31	0.370	2.625
5304	123999	F9IVw	6173 (1)	-0.07	0.541	0.582	0.29	0.44	0.73	1.30	0.347	2.631
5868	141004	G0Vv	5940 (2)	+0.00	0.604	0.672	0.32	0.51	0.83	1.38	0.384	2.606
5914	142373	F8V	5861 (1/2)	-0.43	0.563	0.615	0.32	0.48	0.80	1.53	0.381	2.601
5933	142860	F6V	6246 (2)	-0.14	0.478	—	0.24	0.49	0.73	1.20	0.321	2.632
5986	144284	F8IV	6147 (1)	+0.20	0.528	0.590	0.25	0.45	0.70	1.24	0.354	2.639
6623	161797	G5IV	5496 (1)	+0.03	0.758	0.856	0.38	0.53	0.91	1.65	0.464	2.614
7061	173667	F6V	6368 (1)	-0.09	0.483	0.502	0.26	0.39	0.65	1.10	0.314	2.654
7602	188512	G8IVv	5080 (1)	-0.22	0.855	0.984	0.49	0.66	1.15	2.01	0.523	2.554
7957	198149	K0IV	4997 (1)	-0.29	0.912	1.065	0.49	0.67	1.16	2.15	0.553	—
8181	203608	F6V	6065 (2)	-0.84	0.494	0.522	0.30	0.47	0.77	1.31	0.335	2.618

derivation of IRFM T_{eff} values. In Table A.1 we also list the [Fe/H] measurements and photometry used in the calibrations. As in section 2, strong preference was given to the series of papers by Olsen and co-authors as sources of the $(b - y)$ indices. Sources of these data are given in detail in Table A.2. We have selected 18 stars from Saxner & Hammarbäck (1985) and 23 stars from Blackwell et al. (1991), with 5 stars in common, totalling 36 stars: T_{eff} s for the common stars between these two sources agree within a mean value of 0.8%, and straight averages were used in these cases. All objects have FGK-types and are classified as dwarfs or subgiants (surface gravities confirm this status in all cases); they span approximately a $5000\text{K} \leq T_{\text{eff}} \leq 6500\text{K}$ range, the range in metallicity being $-0.4 \leq [\text{Fe}/\text{H}] \leq +0.3$, with a modest extension to more metal-poor stars; and are close enough that reddening corrections are unnecessary. These atmospheric parameter ranges bracket those of our solar analog and solar twin candidates perfectly.

Blackwell & Lynas-Gray (1994) and Megéssier (1994) discuss discrepancies between the use of older MARCS models and more up-to-date ATLAS models in the deriving of IRFM T_{eff} s. These offsets might amount to $\sim 1\%$ at the extremes of the main sequence, but were found to be much smaller for solar-type stars. Differences between the T_{eff} values of Blackwell & Lynas-Gray (1994) and Blackwell et al. (1991) average $+10 \pm 30$ K, which is inconsequential to our purposes. Moreover, we show below that the calibrations derived here are in very good agreement with recent ones widely cited in the literature. Casagrande et al. (2006) have discussed systematic differences between MARCS and ATLAS models and conclude that while good agreement is found in the visible, in the IR offsets still remain and may be traceable to lingering uncertainties in the absolute flux calibration of Vega, which they regard as a factor still influencing the accuracy of IRFM T_{eff} determinations.

Table 2. Table A.2. References for the $uvby\beta$ photometry and $[\text{Fe}/\text{H}]$ of Table 13.

HR	$(b - y)$	β	$[\text{Fe}/\text{H}]$
33	Grönbech & Olsen (1976)	Grönbech & Olsen (1977)	Balachandran (1990)
98	Crawford et al. (1970)	Heck & Manfroid (1980)	Abia et al. (1988)
244	Strömberg & Perry (1965)	Crawford et al. (1966)	Lambert et al. (1991)
417	Strömberg & Perry (1965)	Crawford et al. (1966)	–
458	Reglero et al. (1987)	Olsen (1983)	Boesgaard & Lavery (1986)
483	Strömberg & Perry (1965)	Crawford et al. (1966)	Clegg et al. (1981)
509	Olsen (1983)	Olsen (1983)	Arribas & Crivellari (1989)
544	Strömberg & Perry (1965)	Crawford et al. (1966)	Balachandran (1990)
740	Grönbech & Olsen (1976)	Olsen (1983)	Balachandran (1990)
799	Strömberg & Perry (1965)	Crawford et al. (1966)	Clegg et al. (1981)
818	Crawford et al. (1970)	Crawford et al. (1970)	Luck & Heiter (2005)
937	Crawford & Barnes (1970)	Crawford et al. (1966)	Chen et al. (2000)
996	Olsen (1983)	Olsen (1983)	Cayrel de Strobel & Bontolila (1989)
1101	Olsen (1983)	Grönbech & Olsen (1977)	Nissen & Edvardsson (1992)
1325	Olsen (1983)	Schuster & Nissen (1988)	Steenbock (1983)
1543	Olsen (1983)	Olsen (1983)	Clegg et al. (1981)
1729	Crawford & Barnes (1970)	Crawford et al. (1966)	Friel & Boesgaard (1992)
1983	Olsen (1983)	Olsen (1983)	Cayrel de Strobel et al. (1988)
2047	Warren & Hesser (1977)	Olsen (1983)	Boesgaard & Friel (1990)
2943	Crawford & Barnes (1970)	Crawford et al. (1966)	Steffen (1985)
4054	Olsen (1983)	Crawford et al. (1966)	Thévenin et al. (1986)
4540	Olsen (1983)	Olsen (1983)	Nissen & Edvardsson (1992)
4785	Warren & Hesser (1977)	Warren & Hesser (1977)	Boesgaard & Lavery (1986)
5072	Manfroid & Sterken (1987)	Crawford et al. (1966)	da Silva et al. (2012)
5185	Manfroid & Sterken (1987)	Crawford et al. (1966)	Thévenin et al. (1986)
5235	Warren & Hesser (1977)	Grönbech & Olsen (1977)	Clegg et al. (1981)
5304	Olsen (1983)	Crawford et al. (1966)	Balachandran (1990)
5868	Olsen (1983)	Olsen (1983)	Boesgaard & Lavery (1986)
5914	Olsen (1983)	Crawford et al. (1966)	Boesgaard & Lavery (1986)
5933	Reglero et al. (1987)	Olsen (1983)	Boesgaard & Lavery (1986)
5986	Warren & Hesser (1977)	Crawford et al. (1966)	Boesgaard & Lavery (1986)
6623	Bond (1970)	Heck (1977)	McWilliam (1990)
7061	Strömberg & Perry (1965)	Reglero et al. (1987)	Boesgaard & Friel (1990)
7602	Olsen (1983)	Stokes (1972)	Edvardsson (1988)
7957	Bond (1970)	Bond (1970)	McWilliam (1990)
8181	Olsen (1983)	Olsen (1983)	Zhao & Magain (1991)

Our calibrations aim derive empirical T_{eff} relations as a function of the most commonly employed photometric colors and additionally, at calibrating the metallicity dependency of the blanketing-sensitive color indices precisely, by using exclusively spectroscopically derived $[\text{Fe}/\text{H}]$ values. The literature was searched for spectroscopic metallicity determinations based on high-resolution spectra and employing a large number of Fe I lines. The $[\text{Fe}/\text{H}]$ values were corrected to full consistency to the T_{eff} (IRFM) scale: for this we used the $\Delta[\text{Fe}/\text{H}]/\Delta T_{\text{eff}}$ provided by the authors themselves, when available, or else the representative value of -0.06 dex for 100K, to correct $[\text{Fe}/\text{H}]$ as a function of the difference between the T_{eff} adopted in the spectroscopic analysis and the IRFM T_{eff} for each star. These $[\text{Fe}/\text{H}]$ values have considerable heterogeneity in what concerns observational data and methods of analysis and part of this heterogeneity should be removed by the correction to the common T_{eff} (IRFM) scale, besides realizing full consistency with the metallicities we derived in section 5.1 for our solar-analog and twin candidates, which are strictly tied to the photometric T_{eff} scale.

The calibrations and comparison to other authors

Our calibrations of T_{eff} against various color indices in widespread use are given in figures A.1 to A.8, along with their

(non-exhaustive) comparisons with published results in wide use. As expected, the data points define tight correlations with little scatter. We tested for possible trends in the correlations with $[\text{Fe}/\text{H}]$ and $\log g$, and in all cases surface gravity did not affect the calibrations, as expected from the quite narrow range of this parameter among our sample. Some colors are clearly affected, however, by blanketing effects to different degrees, even in our narrow T_{eff} and $[\text{Fe}/\text{H}]$ range. Below we give details on the functional forms of the adopted calibrations and their comparison with the literature. We performed two experiments concerning the use of homogenized values from the literature as compared to those selected from individual references. The first one concerns the $(b - y)$ and β photometry, and we tested the use in the calibrations of values taken from individually selected papers compared to mean values given by Hauck & Mermilliod (1998, 1990). The other test involved comparing the calibrations obtained with $[\text{Fe}/\text{H}]$ taken from selected works as opposed to mean values from $[\text{Fe}/\text{H}]$ catalogs (Cayrel de Strobel et al. 2001). For the photometry, significantly tighter regressions and smaller errors in the coefficients were attained when critically selected values from the literature were employed. A similar yet less clear-cut result was obtained for $[\text{Fe}/\text{H}]$. We therefore conclude that catalogs of homogenized values, while extremely helpful, should be used with some care. Not all possible comparisons to recent literature are shown in the plots in order not

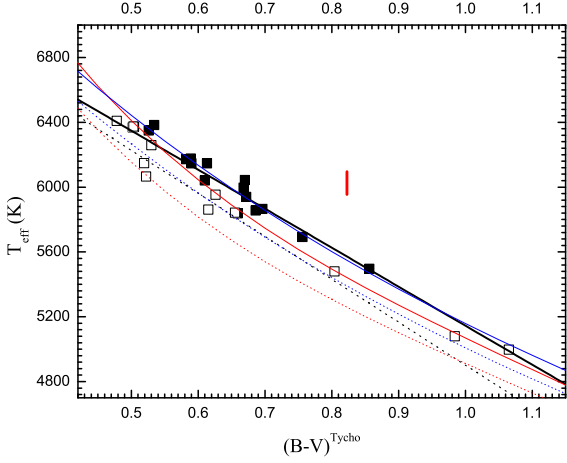


Fig. 2. Figure A.2. The same as Fig. A.1 for the $(B - V)_{\text{Tycho}}$ index: the red and blue lines are the relations of Ramírez & Meléndez (2005b) and Casagrande et al. (2010), respectively.

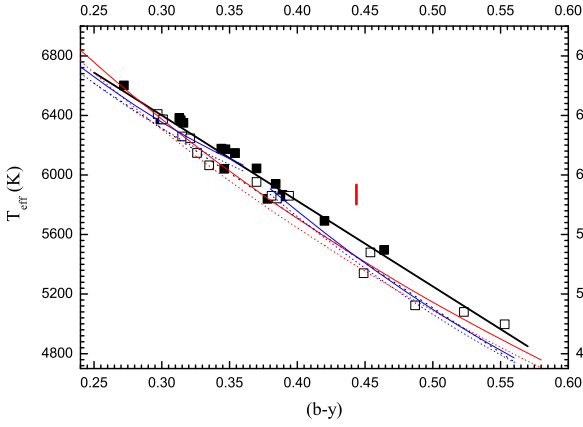


Fig. 3. Figure A.3. The same as Fig. A.1 for the $(b - y)$ index: the red and blue lines are the relations of Alonso et al. (1996) and Blackwell & Lynas-Gray (1998), respectively.

to clutter the diagrams unnecessarily, but relevant remarks are given in the text.

In figures A.1 to A.8 the sample is stratified in two $[\text{Fe}/\text{H}]$ intervals separated by $[\text{Fe}/\text{H}] = -0.10$. The necessity of a $[\text{Fe}/\text{H}]$ term is clear in the Paschen continuum colors, and for the $(B - V)_{\text{Johnson}}$, $(B - V)_{\text{Tycho}}$ and $(b - y)$ regressions we have adopted the same functional relationship as in Saxner & Hammarbäck (1985). For the $(R - I)_{\text{Johnson}}$, $(V - R)_{\text{Johnson}}$ and $(V - I)_{\text{Johnson}}$ regressions, a linear form was found satisfactory, and no $[\text{Fe}/\text{H}]$ term was necessary, while for $(V - K)_{\text{Johnson}}$, and β second-order functions improved the regressions significantly, and also no $[\text{Fe}/\text{H}]$ trends appear. As a formal estimate of the uncertainties, in figures 8 to 15 we plot an error bar quadratically composed of the standard deviations of our regressions and a 2% formal error on the T_{eff} s used for the calibrations (as estimated by Casagrande et al. 2006). While probably underestimating the total error budget, since these two error sources are not independent, this estimate should properly ac-

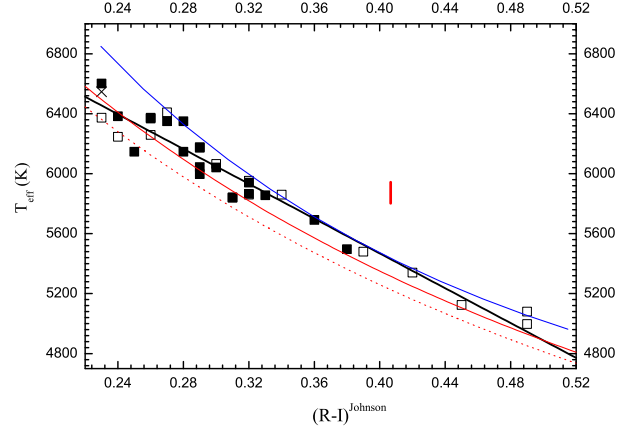


Fig. 4. Figure A.4. The same as Fig. A.1 for the $(R - I)_{\text{Johnson}}$ index. The cross stands for HR 417, without known $[\text{Fe}/\text{H}]$. The black full line is our calibration, the blue line that of Casagrande et al. (2006), and the red full and dotted lines follow the same $[\text{Fe}/\text{H}]$ convention as Fig. A.1 for the calibration of Alonso et al. (1996).

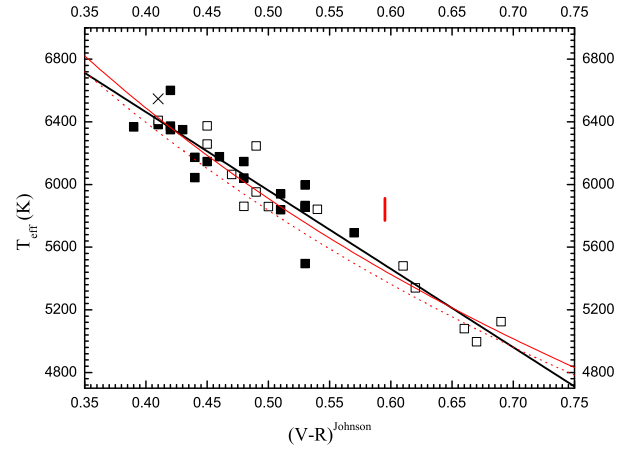


Fig. 5. Figure A.5. The same as Fig. A.4 for the $(V - R)_{\text{Johnson}}$ index: the red full and dotted lines follow the same $[\text{Fe}/\text{H}]$ convention as Fig. A.1 for the calibration of Alonso et al. (1996).

count for differences between T_{eff} scales from different authors, as well as the internal uncertainty in our regressions.

The corresponding regressions are given below, where we also provide the uncertainties in the coefficients, the standard deviation of the fit, and the number of stars employed in each regression:

$$T_{\text{eff}} = 7747 - 3016 (B - V)_{\text{Johnson}} (1 - 0.15 [\text{Fe}/\text{H}])$$

$$\pm 58 \quad \pm 100 \quad \pm 0.04$$

$$\sigma = 65 \text{ K} \quad (36 \text{ stars})$$

$$T_{\text{eff}} = 7551 - 2406 (B - V)_{\text{Tycho}} (1 - 0.20 [\text{Fe}/\text{H}])$$

$$\pm 57 \quad \pm 88 \quad \pm 0.05$$

$$\sigma = 64 \text{ K} \quad (31 \text{ stars})$$

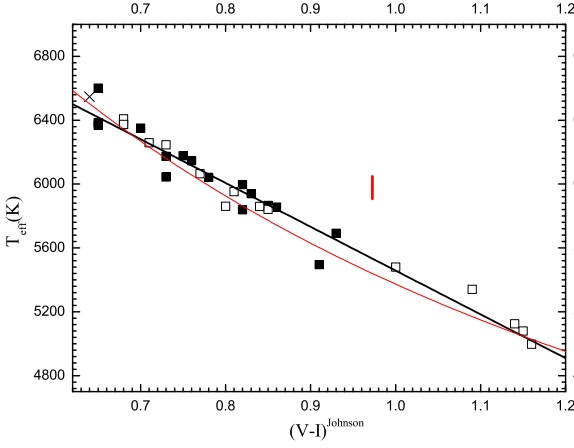


Fig. 6. Figure A.6. The same as Fig. A.4 for the $(V - I)^{\text{Johnson}}$ index. The red line is the calibration of Alonso et al. (1996).

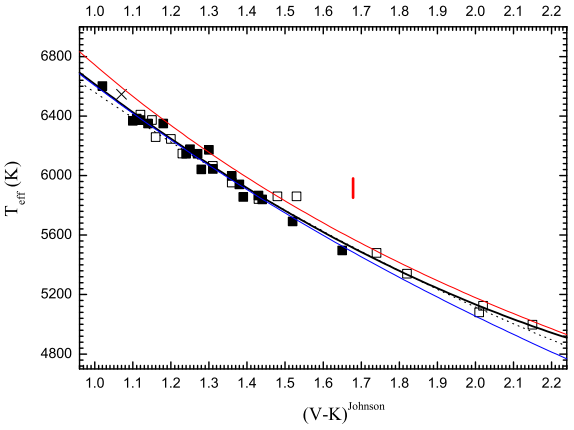


Fig. 7. Figure A.7. The same as Fig. A.4 for the $(V - K)^{\text{Johnson}}$ index. The black full, black dotted, red, and blue lines correspond to the calibrations of this work, Blackwell & Lynas-Gray (1998), Masana et al. (2006), and Alonso et al. (1996), respectively.

$$T_{\text{eff}} = 8124 - 5743(b - y)^F(1 - 0.10[\text{Fe}/\text{H}])$$

$$\pm 58 \quad \pm 156 \quad \pm 0.02$$

$$\sigma = 55 \text{ K} \quad (36 \text{ stars})$$

$$T_{\text{eff}} = 8481 - 6516(b - y)^G(1 - 0.09[\text{Fe}/\text{H}])$$

$$\pm 67 \quad \pm 177 \quad \pm 0.02$$

$$\sigma = 58 \text{ K} \quad (36 \text{ stars})$$

$$T_{\text{eff}} = 7790 - 5805(R - I)^{\text{Johnson}}$$

$$\pm 80 \quad \pm 249$$

$$\sigma = 100 \text{ K} \quad (35 \text{ stars})$$

$$T_{\text{eff}} = 8465 - 5005(V - R)^{\text{Johnson}}$$

$$\pm 139 \quad \pm 276$$

$$\sigma = 125 \text{ K} \quad (35 \text{ stars})$$

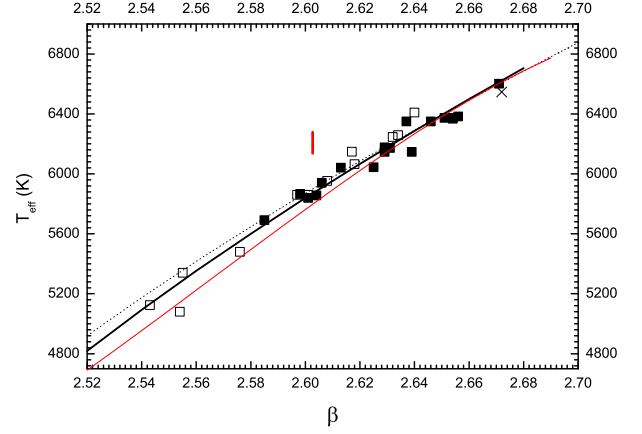


Fig. 8. Figure A.8. The same as Fig. A.4 for the β index. The black full, black dotted, and red lines stand for the calibrations of this work, Saxner & Hammarbäck (1985), and Alonso et al. (1996) respectively.

$$T_{\text{eff}} = 8234 - 3523(V - I)^{\text{Johnson}}$$

$$\pm 75 \quad \pm 116$$

$$\sigma = 77 \text{ K} \quad (35 \text{ stars})$$

$$T_{\text{eff}} = 8974 - 2880(V - K)^{\text{Johnson}} + 440(V - K)^2_{\text{Johnson}}$$

$$\pm 219 \quad \pm 292 \quad \pm 94$$

$$\sigma = 50 \text{ K} \quad (36 \text{ stars})$$

$$T_{\text{eff}} = 11654 \sqrt{\beta - 2.349}$$

$$\pm 182 \quad \pm 0.008$$

$$\sigma = 70 \text{ K} \quad (34 \text{ stars}).$$

Some of these calibrations have already been successfully employed in determining photometric T_{eff} s for solar-type stars (del Peloso et al. 2005; da Silva et al. 2012). We now comment on the agreement of the calibrations shown in figs. 8 to 15 with various published ones in regular use.

In figure A.1, for $(B - V)^{\text{Johnson}}$, a comparison with Alonso et al. (1996) shows good agreement within the 1σ uncertainty we adopt for our target interval of $5000\text{K} \leq T_{\text{eff}} \leq 6500\text{K}$. The results of Casagrande et al. (2006) are in very good agreement with ours in the full T_{eff} range but for a 2σ offset at the hotter end, where their values are hotter. The magnitude of the $[\text{Fe}/\text{H}]$ sensitivity is similar in the three calibrations, but the curvature in our relation is significantly less than in the others, which may be explained by our shorter T_{eff} interval. The Ramírez & Meléndez (2005b) calibration is cooler than in Casagrande et al. by $\sim 100\text{K}$, and more similar to the Alonso et al. one. The latter relation implies a solar $(B - V)$ bluer than ours by about 0.03 mag, while the value implied in Casagrande et al. agrees very well with ours. The comparison of our $(B - V)^{\text{Tycho}}$ calibration in figure A.2 was done with Ramírez & Meléndez (2005b) and Casagrande et al. (2010). There is good agreement with the former at the ends of our T_{eff} range, but at the solar T_{eff} their relation is cooler by $\sim 130\text{K}$. Their sensitivity to $[\text{Fe}/\text{H}]$ is similar to ours, but their regression has a much more pronounced curvature. Very good agreement, however, is found between our relation and that of Casagrande et al. (2010). This color should be more explored more, since little use has been made of it in IRFM T_{eff} calibrations. Its errors are similar to

those of $(B - V)_{\text{Johnson}}$, and its $[\text{Fe}/\text{H}]$ sensitivity is comparable. For $(b - y)$, we separately provide relations for the photometry of the F (Olsen 1983) and G (Olsen 1993) catalogs. We compare in figure A.3 our relation due to the F catalog with those of Blackwell & Lynas-Gray (1998) and Alonso et al. (1996), and the regressions by Blackwell & Lynas-Gray (1998) are given separately for two different ranges separated at $\sim 6000\text{K}$ according to their prescription. These authors do not specify which of the Olsen photometry systems is used in their calibrations. The regression of Alonso et al. (1996) depends on the Strömgren c_1 index: for the comparison we fixed this index at the middle of our interval, namely the value of 18 Sco, a warranted approximation given our narrow $\log g$ interval. Agreement is good particularly at the hotter end and still within 2σ down to $T_{\text{eff}} \sim 5000\text{K}$. The three calibrations have similar curvatures in this range, but our $[\text{Fe}/\text{H}]$ sensitivity is higher than that of Alonso et al. (1996), which in turn is higher than for Blackwell & Lynas-Gray (1998). The solar $(b - y)$ color implied by the Alonso et al. (1996) calibration is bluer than ours by 0.02 mag., while good agreement is found with Blackwell & Lynas-Gray (1998).

The infrared Johnson colors are found to be independent of $[\text{Fe}/\text{H}]$ in our relations but for $(V - K)$. We compare our $(R - I)$ calibration in figure A.4 with those of Alonso et al. (1996) and Casagrande et al. (2006), where the latter relation is independent of $[\text{Fe}/\text{H}]$, while the former is not. The relation of Casagrande et al. (2006) has been transformed from the Cousins to the Johnson system with the prescription given by Bessell (1979). Our results agree very well with Alonso et al. (1996), especially at the ends of our T_{eff} range: near the solar T_{eff} the offset is still within 1σ . The Casagrande et al. (2006) calibration is in good agreement with ours near the solar T_{eff} but is hotter at both ends of our T_{eff} range, particularly near $T_{\text{eff}} = 6500\text{K}$ where the disagreement reaches 2σ . For the Johnson $(V - R)$ and $(V - I)$ colors, we compare respectively in figures A.5 and A.6, our relations to Alonso et al. (1996). For $(V - I)$ we both found no sensitivity to $[\text{Fe}/\text{H}]$, and agreement is good for the full T_{eff} range. For $(V - R)$, the Alonso et al. (1996) relation depends on $[\text{Fe}/\text{H}]$, unlike ours, but again good agreement is found for the full range: however, a larger scatter is seen, and the standard deviation of our fit for this color is the highest. For the Johnson $(V - K)$ color, we compared in figure A.7 our calibrations with those of Alonso et al. (1996), Blackwell & Lynas-Gray (1998), and Masana et al. (2006). Only the Alonso et al. (1996) regression is very slightly $[\text{Fe}/\text{H}]$ -sensitive and we set $[\text{Fe}/\text{H}]$ to the solar value for comparison. The agreement of the three calibrations is very good for the full T_{eff} range, and we note that the relation given by McWilliam (1990) is also compatible with the previously mentioned calibrations in this T_{eff} range.

For the Strömgren β index, we compare our regression with those of Saxner & Hammarbäck (1985) and Alonso et al. (1996) in figure A.8. Not surprisingly, our results are in line with Saxner & Hammarbäck (1985). The calibration of Alonso et al. (1996) is only weakly $[\text{Fe}/\text{H}]$ -dependent and we set $[\text{Fe}/\text{H}] = +0.00$ for the comparison: this calibration also shows good agreement in our T_{eff} range. The β color index, though more difficult to obtain for faint stars due to the narrowness of the filters, has good T_{eff} sensitivity in this range, is reddening-free, and could be explored more for solar-type stars.

Taking into account that IRFM T_{eff} s are accurate to no more than a few percent (Ramírez & Meléndez 2005a; Casagrande et al. 2006), the agreement of our calibrations with many widely adopted recent resources ranges from fair to very good, within a 2σ assessment but for a few cases. In the range

of T_{eff} we are exploring, they provide good internal consistency and collectively enable the derivation of photometric T_{eff} s for solar-type stars, within a reasonable range around the solar atmospheric parameters, with internal errors less than 1%. The external errors of the IRFM T_{eff} scale are, of course, larger by at least a factor of two.

Acknowledgements. This paper is dedicated, *in memoriam*, to Giusa Cayrel de Strobel, for her dedicated pioneering in the subject of solar analogs and twins. G. F. P. M. acknowledges financial support by CNPq grant n° 476909/2006-6, FAPERJ grant n° APQ1/26/170.687/2004, and a CAPES post-doctoral fellowship n° BEX 4261/07-0. R. S. acknowledges a scholarship from CNPq/PIBIC. L. S. thanks CNPq for the grant 30137/86-7. We thank the staff of the OPD/LNA for considerable support in the observing runs needed to complete this project. Use was made of the Simbad database, operated at the CDS, Strasbourg, France, and of NASAs Astrophysics Data System Bibliographic Services. We thank Giusa Cayrel de Strobel, *in memoriam*, Edward Guinan, José Dias do Nascimento Jr., José Renan de Medeiros, and Jeffrey Hall for interesting discussions. We also thank the referee, Dr. Martin Asplund, for suggestions and criticism which considerably improved the paper.

References

- Abia C., Rebolo R., Beckman J.E., & Crivellari L. 1988, A&A, 206, 100
- V. Zh. Adibekyan, V. Zh., Figueira, P., Santos, N. C., Hakobyan, A. A., Sousa, S. G., Pace, G., Delgado Mena, E., Robin, A. C., Israelian, G. & González Hernández, J. I. 2013, A&A, 554, A44
- Alonso, A., Arribas, S., & Martínez-Roger, C. 1996, A&A, 313, 873
- Alvarez-Candal, A., Duffard, R., Lazzaro, D., & Michtchenko, T. 2007, A&A, 459, 969
- Arribas S., & Crivellari L. 1989, A&A, 210, 211
- Asplund, M., Grevesse, N., Jacques Sauval, A. & Scott, P. 2009, Ann. Rev. A&A, 47, 481
- Balachandran S. 1990, ApJ, 354, 310
- Barklem, P. S., Stempels, H. C., Allende Prieto, C., Kochukhov, O. P., Piskunov, N. & O'Mara, B. J. 2002, A&A 385, 951
- Baumann, P., Ramírez, I., Meléndez, J., Asplund, M. & Lind, K. 2010, A&A 519, A87
- Bessell M. S. 1979, PASP, 91, 589
- Blackwell, D.E., & Shallis, M.J. 1977, MNRAS, 180, 177
- Blackwell D.E., Booth A.J., Legget S.K., Mountain C.M., & Selby M.J. 1986, MNRAS, 221, 427
- Blackwell D. E., Petford A. D., Arribas S., Haddock D. J., & Selby M. J. 1990, A&A, 232, 396
- Blackwell D.E., Lynas-Gray A.E., & Petford A.D. 1991, A&A, 245, 567
- Blackwell, D.E., & Lynas-Gray, A.E. 1994, A&A, 282, 899
- Blackwell, D.E., & Lynas-Gray, A.E. 1998, A&A Supp., 129, 505
- Boesgaard A.M., & Friel E. 1990, ApJ, 351, 467
- Boesgaard A.M., & Lavery R.J. 1986, ApJ, 309, 762
- Bond H. E. 1970, ApJS, 22, 117
- Casagrande, L., Portinari, L., & Flynn, C. 2006, MNRAS, 373, 13
- Casagrande, L., Ramírez, I., Meléndez, J., Bessell, M. 2010, & Asplund, M. 2010, A&A, 512, A54
- Cayrel, R., Cayrel de Strobel, G., & Campbell, B. 1985, A&A, 146, 249
- Cayrel R., Cayrel de Strobel G., & Campbell B. 1988, IAU Symposium 132, p. 449
- Cayrel de Strobel, G., Knowles, N., Hernandez, G., & Bentolila, C. 1981, A&A, 94, 1
- Cayrel de Strobel, G., & Bentolila, C. 1989, A&A, 211, 324
- Cayrel de Strobel, G. 1996, A&ARv, 7, 243
- Cayrel de Strobel G., Soubiran C., & Ralite, N. 2001, A&A, 373, 159
- Chen, Y. Q., Nissen, P. E., Zhao, G., Zhang, H. W., Benoni, & T. 2000, A&AS, 141, 491
- Clegg R.E.S., Lambert D.L., & Tomkin J. 1981, ApJ, 250, 262
- Crawford, D.L., Barnes, J.V., Faure, B.Q., & Golson, J.C. 1966, AJ, 71, 709
- Crawford, D.L., Barnes, J.V., & Golson, J.C. 1970, AJ, 75, 624
- Crawford D.L., & Barnes J.V. 1970, AJ, 75, 978
- da Silva, R. O., Porto de Mello, G. F., Milone, A. C., da Silva, L., Ribeiro, L. S. & Rocha-Pinto, H. J. 2012, A&A, 542, A84
- del Peloso E. F., da Silva L., & Porto de Mello G. F. 2005, A&A, 434, 275
- do Nascimento Jr, J.D., Castro, M., Meléndez, J., et al. 2009, A&A, accepted
- Edvardsson B. 1988, A&A, 190, 148
- Edvardsson, B., Andersen, J., Gustafsson, B., et al. 1993, A&A, 275, 101
- ESA 1997, The Hipparcos and Tycho catalogs, SP-1200

- Feldman P. D., Cochran A.m & Combi M. R. 2004, *Spectroscopic Investigations of Fragment Species in the Coma*, in Comets II, eds. M. C. Festou, H. U. Keller, H. A. Weaver, The University of Arozina Press in collaboration with the Lunar Planetary Institute
- Fesenko, B. I. 1994, *Astronomy Reports*, 38, 266
- Flower, P.J. 1996, *ApJ*, 469, 355
- Friel E., & Boesgaard A.M. 1992, *ApJ*, 387, 170
- Friel, E., Cayrel de Strobel, G., Chmielewski, Y., et al. 1993, *A&A*, 274, 825
- Fuhrmann, K., Axer, M., & Gehren, T. 1993, *A&A*, 271, 451
- Galeev, A.I., Bikmaev, I.F., Musaev, F.A., & Galazutdinov, G.A. 2004, *Astronomy Reports*, 48, 429
- Gancarz, A.K., & Wasserburg, G. J. 1977, *Geochimica et Cosmochimica Acta*, 41, 1283
- Ghezzi, L., Cunha, K., Smith, V.V., & de la Reza, R. 2010, *ApJ*, 724, 154
- Glass I. S. 1974, *MNASSA*, 33, 53
- Glushneva, I.N., Shenavrin, V.I., & Roshchina, I.A. 2000, *Astronomy Reports*, 44, 254
- Gonzalez, G., Bronwlee, D., & Ward, P. 2001, *Icarus*, 152, 185
- Gray, D.F. 1992, *PASP*, 104, 1035
- Gray, D.F. 1994, *PASP*, 106, 1248
- Grevesse, N., & Noels, A., in N. Prantzos, E. Vangioni-Flam & M. Cassé (eds.), *Origin and Evolution of the Elements*, p. 14, Cambridge Univ. Press, Cambridge
- Grönbech, B., & Olsen, E.H. 1976, *A&AS*, 25, 213
- Grönbech, B., & Olsen, E.H. 1977, *A&AS*, 27, 443
- Grudzińska S. & Barbon R. 1968, *Acta Astronomica*, 18, 323
- Gustafsson, B. 1998, *Space Science Reviews*, 85, 419
- Gustafsson, B., Edvardsson, B., Eriksson, K., et al. 2008, *A&A*, 486, 951
- Guenther, D.B. 1989, *ApJ*, 339, 1156
- Hall, J.C., & Lockwood, G.W. 2000, *ApJ*, 545, L43
- Hall, J.C., Henry, G.W., & Lockwood, G.W. 2007, *AJ*, 133, 2206
- Hall J. C., Henry G. W., Lockwood G. W., Skiff B. A., & Saar S. H. 2009, *AJ*, 138, 312
- Hardorp, J. 1982, *A&A*, 105, 120
- Hauck B., & Mermilliod M. 1990, *A&AS*, 86, 107
- Hauck B., & Mermilliod M. 1998, *A&AS*, 129, 431
- Hayes, D.S. 1985, *IAU Symposium 111, Calibration of Fundamental Stellar Quantities*, eds. D. S. Hayes et al. (Dordrecht, Reidel), p. 225
- Heck A. 1977, *A&AS*, 27, 47
- Heck A., & Manfroid J. 1980, *A&AS*, 42, 311
- Hoffleit, D., & Jaschek, C. 1991, *The Bright Star Catalogue*, 5th edition
- Hoffleit, D. 1991, *Supplement to the Bright Star Catalogue*
- Holmberg, J. Flynn, C., & Portinari, L. 2006, *MNRAS*, 367, 449
- Israelian, G., Santos, N.C., Mayor, M., & Rebolo, R. 2004, *A&A*, 414, 601
- Israelian, G., Delgado Mena, E., Santos, N. C., Sousa, S. G., Mayor, M., Udry, S., Domínguez Cerdeña, C., Rebolo, R., Randich, S. 2009, *Nature*, vol. 462, issue 7270, p. 189
- Johnson H. L. 1964, *Bol. Obs. Ton. Tacubaya*, 3, 305
- Johnson H. L., Mitchel I. R., Iriarte B., Wísniowski W. Z. 1966, *Comm. Lunar. Plan. Lab.*, 4, 99
- Johnson H. L., MacArthur J. W., Mitchell R. I. 1968, *ApJ*, 152, 465
- Kaufer, A., Stahl, O., Tubbesing, S., et al. 1999, *The Messenger*, 95, 8
- King, J.R., Boesgaard, A.M., & Schuler, S.C. 2005, *AJ*, 130, 2318
- Kurucz, R.L., Furenlid, I., Brault, J., & Testerman, L. 1984, *Solar Flux Atlas from 296 to 1300 nm*, National Solar Observatory
- Lambert D.L., Heath J.E., & Edvardsson B. 1991, *MNRAS*, 253, 610
- Leitch, E.M., & Vasisht, G. 1998, *New Astronomy*, 3, 51
- Lépine, J.R.D., Mishurov, Y.N., & Dedikov, S.Y. 2001, *ApJ*, 546, 234
- Lockwood G. W., Skiff B. A., Henry G. W., Henry S., Radick R. R., Baliunas S. L., Donahue R. A., & Soon W. 2007, *ApJS*, 171, 260
- Luck, R.E., & Heiter, U. 2005, *AJ*, 129, 1063
- Luck, R.E., & Heiter, U. 2006, *AJ*, 131, 3069
- Lyra, W., & Porto de Mello, G.F. 2005, *A&A*, 431, 329
- Manfroid J., & Sterken C. 1987, *A&AS*, 71, 539
- Masana, E., Jordi, C., & Ribas, I. 2006, *A&A*, 313, 873
- McNamara, D.H., & Powell, J.M. 1985, *PASP*, 97, 1101
- McWilliam A. 1990, *ApJS*, 74, 1075
- Megéssier C. 1994, *A&A*, 289, 202
- Meléndez, J., Dodds-Eden, K., & Robles, J.A. 2006, *ApJ*, 641, L133
- Meléndez, J., & Ramírez, I. 2007, *ApJ*, 669, L89
- Meléndez, J., Schuster, W. J., Silva, J. S., Ramírez, I., Casagrande, L., & Coelho, P. 2010, *A&A*, 522, A98
- Meléndez J., Bergemann M., Cohen J. G., Endl M., Karakas A. I., Ramírez I., Cochran W. D., Yong D., MacQueen P. J., Kobayashi C., & Asplund M. 2012, *A&A*, 543, A29
- Meylan, T., Furenlid, I., Wigss, M.S., & Kurucz, R.L. 1993, *ApJS*, 85, 163
- Milani, G.A., Szabó, G.M., Sosteroa, G., et al. 2006, *Icarus*, 187, 276
- Moore, C.E., Minnaert, M.M., & Houtgast, J. 1966, *The Solar Spectrum from 2935 Å to 8770 Å*, Nat. Bur. Std., U.S. Monograph 61
- Neckel, H. 1986, *A&A*, 159, 175
- Nieva, M.-F. & Przybilla, N. 2012, *A&A*, 539, A143
- Nissen P.E., & Edvardsson B. 1992, *A&A*, 261, 255
- Olsen, E.H. 1983, *A&AS*, 54, 55
- Olsen, E.H. 1993, *A&AS*, 102, 89
- Olsen, E.H. 1994, *A&AS*, 104, 429
- Olsen, E.H., *A&AS*, 106, 257
- Pace, G., & Pasquini, L. 2004, *A&A*, 426, 1021
- Pasquini, L., Liu, Q., & Pallavicini, R. 1994, *A&A*, 287, 191
- Paulson, D.B., Sneden, C., & Cochran, W.D. 2003, *AJ*, 125, 3185
- Pereira, T. M. D., Asplund, M., Collet, R., Thaler, I., Trampedach, R. & Leenaerts, J. 2013, *A&A*, 554, A118
- Porto de Mello, G.F., & da Silva, L. 1997, *ApJ*, 482, L89
- Porto de Mello, G.F., del Peloso, E.F., & Ghezzi, L. 2006, *Astrobiology*, 6, 308
- Porto de Mello, G.F., Lyra W., & Keller G. R. 2008, *A&A*, 488, 653
- Porto de Mello, G. F., Lépine, J. R., & da Silva Dias, W. 2009, *Proceedings, Bioastronomy 2007: Molecules, Microbes and Extraterrestrial Life*, Astronomical Society of the Pacific Conference Series, eds. Karen J. Meech, Jacqueline V. Keane, Michael J. Mumma, Janet L. Siefert, and Dan J. Werthimer, vol. 420, pp. 349-352
- Radick, R.R., Lockwood, G.W., Skiff, G.W., & Baliunas, S. L. 1998, *ApJS*, 118, 239
- Ramírez, I., & Meléndez, J. 2005a, *ApJ*, 626, 446
- Ramírez, I., & Meléndez, J. 2005b, *ApJ*, 626, 465
- Ramírez, I., Allende-Prieto, C., & Lambert, D.L. 2007, *A&A*, 465, 271
- Reglero V., Giménez A., de Castro E., & Fernandez-Figueroa M.J. 1987, *A&AS*, 71, 421
- Rocha-Pinto, H.J., & Maciel, W.J. 1996, *MNRAS*, 279, 447
- Rufener, F. 1988, *Catalogue of Stars Measured in the Geneva Observatory Photometric System*, Geneva Observatory
- Saxner, M., & Hammarbäck, G. 1985, *A&A*, 151, 372
- Schaller, G., Schaerer, D., Meynet, G., & Maeder, A. 1992, *A&AS*, 96, 269
- Schaerer, D., Meynet, G., Maeder, A., & Schaller, G. 1993, *A&AS*, 98, 253
- Schuster, W.J., & Nissen, P.E. 1988, *A&AS*, 73, 225
- Segura, A., Krellove, K., Kasting, J.F., Sommerlatt, D., Meadows, V., Crisp, D., Cohen, M., & Mlawer, E. 2003, *Astrobiology*, 3, 689
- Selby M. J., Hepburn I., Blackwell D. E., Booth A. J., Haddock D. J., Arribas S., Legget S. K., & Mountain C. M. 1988, *A&AS*, 74, 127
- Soubiran, C., & Triaud, A. 2004, *A&A*, 418, 1089
- Steenbock W. 1983, *A&A*, 126, 325
- Steffen, M. 1985, *A&AS*, 59, 403
- Stokes N.R. 1972, *MNRAS*, 159, 165
- Strömgren B., & Perry C.L. 1965, *Institute for Advanced Study*, Princeton N.J. (unpublished)
- Takeda, Y., Kawanoto, S., Honda, S., Ando, H., & Sakurai, T. 2007, *A&A*, 468, 663
- Tarter, J. 2001, *ARA&A*, 39, 511
- Thévenin F., Vauclair S., & Vauclair G. 1986, *A&A*, 166, 216
- Tüg, H., & Schmidt-Kaler, T. 1982, *A&A*, 105, 400
- Warren W.H., & Hesser J.L. 1977, *ApJS*, 34, 115
- Yong, D., Lambert, D. L., Allende Prieto, C. & Paulson D. B. 2004, *ApJ*, 603, 697
- Zhao G., & Magain P. 1991, *A&A*, 244, 425